LEVEL II

(13)

AD A109405

USAAEFA PROJECT 79-02-2

HELICOPTER ICING SPRAY SYSTEM (HISS) NOZZLE IMPROVEMENT EVALUATION

FINAL REPORT

BY

DAUMANTS BELTE
PROJECT ENGINEER

12 53

SEPTEMBER 1981

Approved for public release; distribution unlimited.

UNITED STATES ARMY AVIATION ENGINEERING FLIGHT ACTIVITY
EDWARDS AIR FORCE BASE, CALIFORNIA 93523

DISCLAIMER NOTICE

The findings of this report are not to be construed as an official Department of the Army position unless so designated by other authorized documents.

DISPOSITION INSTRUCTIONS

Destroy this report when it is no longer needed. Do not return it to the originator.

TRADE NAMES

The use of trade names in this report does not constitute an official endorsement or approval of the use of the commercial hardware and software.

UNCLASSIFIED
SECURITY CLASSIFICATION OF THIS PAGE (When Data Entered)

REPORT DOCUMENTATION PAGE		READ INSTRUCTIONS BEFORE COMPLETING FORM
1. REPORT NUMBER USAAEFA ~~PROJECT~~ NO. 79-02-02	2. GOVT ACCESSION NO. AD-A109405	3. RECIPIENT'S CATALOG NUMBER
4. TITLE (and Subtitle) HELICOPTER ICING SPRAY SYSTEM (HISS) NOZZLE IMPROVEMENT EVALUATION		5. TYPE OF REPORT & PERIOD COVERED FINAL REPORT SEPT 1981
		6. PERFORMING ORG. REPORT NUMBER
7. AUTHOR(s) DAUMANTS BELTE		8. CONTRACT OR GRANT NUMBER(s)
9. PERFORMING ORGANIZATION NAME AND ADDRESS US ARMY AVIATION ENGINEERING FLIGHT ACTIVITY EDWARDS AFB, CALIFORNIA 93523		10. PROGRAM ELEMENT, PROJECT, TASK AREA & WORK UNIT NUMBERS EKOPW003EKEC
11. CONTROLLING OFFICE NAME AND ADDRESS US ARMY AVIATION RESEARCH AND DEVELOPMENT COMMAND ST. LOUIS, MISSOURI 63120		12. REPORT DATE SEPTEMBER 1981
		13. NUMBER OF PAGES 52
14. MONITORING AGENCY NAME & ADDRESS(if different from Controlling Office)		15. SECURITY CLASS. (of this report) UNCLASSIFIED
		15a. DECLASSIFICATION/DOWNGRADING SCHEDULE

16. DISTRIBUTION STATEMENT (of this Report)

17. DISTRIBUTION STATEMENT (of the abstract entered in Block 20, if different from Report)

18. SUPPLEMENTARY NOTES

19. KEY WORDS (Continue on reverse side if necessary and identify by block number)

Artificial Icing	Median Volumetric Diameter (MVD)
Cloud Composition	Nozzle Performance
Drop Size Distribution	Particle Measuring Spectrometers
Helicopter Icing Spray System (HISS)	Spray Atomizers
Liquid Water Content (LWC)	

20. ABSTRACT (Continue on reverse side if necessary and identify by block number)

The U.S. Army Aviation Engineering Flight Activity (USAAEFA) operates a modified CH-47C helicopter as an airborne spray tanker to create a simulated icing test environment. This Helicopter Icing Spray System (HISS) was modified in 1979 to improve its spray cloud characteristics with respect to uniformity of liquid water content (LWC) and reduction of drop size median volumetric diameter (MVD). The existing atomizers on the spray boom assembly were replaced by Sonic Development Corporation model 125-H "Sonicore" nozzles. A UH-1H helicopter equipped with particle measuring spectrometers conducted in-flight sampling and calibration of the modified HISS spray cloud during Jan - Mar 1980 at St. Paul, Minnesota in conjunction with other helicopter icing

DD FORM 1 JAN 73 1473 EDITION OF 1 NOV 65 IS OBSOLETE

UNCLASSIFIED
SECURITY CLASSIFICATION OF THIS PAGE (When Data Entered)

tests. Average cross sectional dimensions of the present spray cloud are estimated as 36 ft wide and 8 ft deep. Usable values of cloud LWC in excess of 1 gram per cubic meter with a drop size MVD range of 20 to 35 microns could be generated at a 90 knot airspeed. This represents a vast improvement over the artificial cloud of previous years, and overlaps the MVD range representative of natural icing clouds. Test aircraft ice formations produced with the artificial cloud compared favorably with those seen in the natural environment.

DEPARTMENT OF THE ARMY

HQ, US ARMY AVIATION RESEARCH AND DEVELOPMENT COMMAND
4300 GOODFELLOW BOULEVARD, ST. LOUIS, MO 63120

DRDAV-D

SUBJECT: Directorate for Development and Qualification Position on the Final Report of USAAEFA Project No. 79-02-2, Helicopter Icing Spray System (HISS) Nozzle Improvement Evaluation

SEE DISTRIBUTION

1. The purpose of this letter is to establish the Directorate for Development and Qualification position on the subject report.

2. The Directorate agrees with the report conclusion and recommendations. The report documents the incorporation of the Sonic Development Model 125-HB nozzles which significantly improved the HISS spray cloud as well as the reduction in the boom induced helicopter vibrations. However, the cloud size was reduced to 36 feet width by 8 feet depth due to elimination of the nozzles from the boom outriggers. To correct the preceding, a contract was negotiated with Boeing Vertol to improve the existing HISS air supply capability by incorporating a Solar T-62T-40C2 bleed air auxiliary power unit (APU). The APU installation will be provided to the US Army Aviation Engineering Flight Activity (USAAEFA) along with the necessary valving, plumbing controls and associated hardware prior to the 1981/1982 icing season. Once installed, the APU will provide augmented bleed air to the HISS during spray operations. The added APU mass air flow in conjunction with the engine bleed air should result in increasing the cloud width from 36 feet to 60 feet. Future improvements to the HISS will be conducted under a phase 2 effort when funded. The goals of the phase 2 are to further increase the HISS cloud size to a 30 ft depth and provide a flow capability up to 3 g/m^3 liquid water content (LWC).

FOR THE COMMANDER:

CHARLES C. CRAWFORD, JR.
Director of Development and Qualification

Accession For	
NTIS GRA&I	X
DTIC TAB	☐
Unannounced	☐
Justification	
By	
Distribution/	
Availability Codes	
Dist	Avail and/or Special
A	

TABLE OF CONTENTS

INTRODUCTION

BACKGROUND

1. The US Army's need for an all-weather operational capability in its helicopter fleet has led to extensive icing qualification tests. Since 1973, the US Army Aviation Engineering Flight Activity (USAAEFA) has used a modified CH-47C helicopter as an airborne spray tanker to create a simulated icing test environment. Previous results indicated that the artificial cloud produced by the Helicopter Icing Spray System (HISS) was not an adequate simulation of the natural icing environment (Reference 1, Appendix A).

2. In 1979 a program was conducted to investigate and implement HISS modifications to improve its spray characteristics and icing simulation capability. This effort included a wind tunnel evaluation of alternate nozzles by Boeing Vertol in the NASA Lewis Icing Research Tunnel (Reference 2, Appendix A). The modification program and additional HISS background are summarized in Reference 3. A test request (Reference 4) issued by the US Army Aviation Research and Development Command (AVRADCOM) combined research requirements of the Applied Technology Laboratory (ATL) and the Federal Aviation Administration (FAA) to conduct an evaluation of ice phobic coatings, collect data in natural icing conditions, and evaluate the modified HISS. A test plan was prepared (Reference 5) to meet these objectives. The ice phobic evaluation and natural icing characteristics are reported in Reference 6; this report summarizes the modified HISS evaluation. Cloud measuring equipment and data processing and analysis for this project were furnished under contract to ATL by Meteorology Research Inc (MRI), and their results are reported in Reference 7.

TEST OBJECTIVE

3. The objective of this test was to evaluate and quantify the inflight spray characteristics of the modified HISS in actual operation by relating artificial cloud liquid water content (LWC) and drop size distribution to water flow rate, distance behind the spray booms, and vertical and horizontal dimensions of the spray cloud.

DESCRIPTION

4. The HISS, further described in Appendix B, is installed in a modified CH-47C helicopter (S/N 68-15814) and consists of an internal water tank and an external spray boom assembly suspended 19 feet beneath the aircraft from a cross-tube through the cargo compartment. Hydraulic actuators rotate the cross tube to raise and lower the boom assembly. Because of gross weight and center of gravity limitations, the aft fuel cells of the helicopter are left empty and only 1400 gallons of water are carried. Both the external boom assembly and internal water supply can be jettisoned in an emergency. For icing tests, a chemical dye is added to the water and imparts a yellow color to the ice.

5. The spray boom consists of two 27 ft center sections, vertically separated by 5 ft, and two 17.6 ft outriggers attached to the upper boom. The outriggers are swept aft 20° and angled down 10°, giving a tip to tip boom width of 60 ft. The spray cloud is generated by pumping water at selected flow rates from the tank to the nozzles on the boom assembly, using aircraft engine compressor bleed air to

atomize the water. The boom is assembled of concentric metal tubing; the inner pipe (1-1/2" diameter) acts as the water supply and leads to 30 manifolds spaced approximately 3 ft apart along the boom exterior; the outer pipe (4" diameter) contains bleed air from the aircraft engines, and is fitted with a total of 172 receptacles on the boom surface. These nozzle receptacles are spaced at 1 ft intervals along the top and bottom of the boom and are staggered to provide alternating upward and downward ejection ports every 6 inches. Sonic Development Corporation Model 125-H Sonicore nozzles were installed for this evaluation.

6. A calibrated outside air temperature probe and a Cambridge dew point hygrometer provide accurate ambient temperature and humidity measurement. An aft-facing radar altimeter is mounted at the rear of the HISS to allow positioning the test aircraft at a known standoff distance. Thermocouples and pressure transducers were installed on the boom assembly at two locations to allow in-flight measurement of pressure and temperature for both boom air and water while spraying, as described in Appendix C.

7. The measurement aircraft used to sample the spray cloud was a JUH-1H helicopter (S/N 70-16318), equipped with an ice protection system (IPS) and test instrumentation as described in Reference 6. Spray cloud measurements were made using onboard particle measuring spectrometers furnished by MRI. Three probes were available, each capable of counting and sizing particles into 15 size classes. These probes and the data reduction methods are described in Reference 7 and Appendixes C and D. The axially scattering probe (ASP) operates over a 3 to 45 micron (μm) diameter range, the cloud particle spectrometer (CPS) over 35 to 300 μm, and the precipitation particle spectrometer (PPS) over 140 to 2100 μm. The ASP was mounted on the left side of the aircraft, and either the CPS or PPS probe on the right side. Horizontal distance between them was 10 ft 10 in.

TEST SCOPE

8. The measurement aircraft conducted in-flight sampling of the HISS spray cloud from 12 Jan to 24 Mar 1980 in the vicinity of St. Paul, Minnesota. A total of 15 flights were conducted behind the HISS for a total of 19.6 hours, used for spray sampling as well as IPS verification in the artificial cloud. Cloud immersion time is not applicable, since numerous in and out of cloud sampling maneuvers were performed on any given flight. Test conditions for flights that included spray sampling are presented in Table 1. In addition to this project the HISS concurrently flew in support of two other icing programs (USAAEFA Projects 79-07, YCH-47D and 79-17, UH-60A), allowing further in-flight evaluation of HISS characteristics.

METHODOLOGY

9. To quantify the HISS spray cloud in terms of LWC and drop size distribution, the measurement aircraft flew in formation behind the HISS, and sampled the drops by maneuvering to immerse the particle measuring spectrometers in the spray plume. A chase helicopter accompanied each flight to observe the measurement aircraft, assist in positioning, and provide airborne still and motion picture photography.

Table 1
Test Conditions[1]

Flt No.	Pressure Altitude (ft)	Outside Air Temp (°C)	Relative Humidity (%)	HISS Configuration	Comments
1	2400	-9.5	26	160 Nozzles including outriggers	IPS[2] checkout
2	2200	-7.0	86		IPS checkout
3	6900	-5.0	71		Spray Calibration[3] - low bleed air pressure noted
4	2500	-21.0	67	Nozzles removed from outriggers	Spray calibration - HISS water pump problems
6	2500	-23.0	57	Water filter installed	Spray calibration - freezing blocks numerous nozzles
7	1800	-14.0	66	Purge air line rerouted	IPS checkout completed
8[5]	1800	-13.5	63	Final configuration - 97 nozzles on center boom section only - outriggers isolated	Spray calibration - residual water freezing in boom
9[5]	1800	-11.5	85		Spray calibration
10[5]	3000 10,000	-9.5 -17.0	90 75		Spray calibration
11	4500	-10.0	55		Spray calibration using PPS[4] probe
12[5]	2500	-10.0	85		Spray calibration - ASP probe iced over
13[5]	2900	-9.5	85		Spray calibration
19	3900	-8.0	55		Spray calibration - MRI probes rechecked
27	3000	-6.0	72		Spray calibration - new ASP installed

[1] HISS Flight condition; 90 KTAS. Water flow rates were varied from 4 to 50 gal/min, standoff distance 150 to 300 ft. Sonic Development Corp. "Sonicore" model 125-H nozzles were installed.
[2] IPS: Ice protection System on the JUH-1H measurement aircraft
[3] Cloud measurements made with an Axially Scattering Probe (ASP) and a Cloud Particle Spectrometer (CPS) furnished by Meteorology Research Inc. (MRI)
[4] PPS: Precipitation Particle Spectrometer, a third probe available from MRI for measuring larger drop sizes
[5] MRI data from these flights used for final analysis of spray cloud characteristics.

10. The target airspeed for these tests was 90 knots true airspeed (KTAS). Standoff distances from the rear of the HISS, as measured by the radar altimeter, were varied from 150 to 300 ft (distance between the spray booms and the radar altimeter at the rear of the HISS was an additional 35 ft).

11. A typical sequence at a given test condition included both vertical and horizontal sweeps through the spray cloud, as well as stabilizing as long as 2 minutes with the probes held approximately centered in the cloud. The measurement aircraft initiated its vertical sweeps from a centered position beneath the cloud, climbing slowly until the probes were above the cloud, and then descending to the starting point. Horizontal sweeps were initiated from the center of the cloud, moving laterally to the left edge, followed by a sweep to the right. Returning to the starting point outside the cloud, the measurement aircraft would then perform additional sweeps or stabilize at points centered in the cloud.

RESULTS AND DISCUSSION

GENERAL

12. A nozzle investigation during 1979 resulted in the selection of Sonic Development Corporation atomizers to replace the existing units on the HISS spray boom. During the 1979-1980 icing season, operational characteristics of the modified HISS were observed and the new spray cloud characteristics were measured. Quantitative measurements of the present artificial cloud show considerable improvement over previous years in consistency of liquid water content and drop size median volumetric diameter, which now overlaps the 10 to 30 μm range representative of natural icing clouds.

SPRAY DEFINITIONS

13. LWC and drop distribution are of primary interest in spray tanker development as they specify the icing cloud composition. LWC is given in units of grams (gm) water per cubic meter (m^3) of air, and the conversion from drop volume to water mass is made using water density as 1 gm/cm^3. Parameters used to characterize drop distributions are the median and mean volume diameters. Median volumetric diameter (MVD) divides the volume of the spray into halves such that half of the total water volume is contained in drops larger and half in drops smaller than this median diameter. The mean diameter is the drop size whose volume is given by dividing the total mass of water by the total number of drops present. Since volume varies as the cube of diameter, a few large drops have a much greater effect on total water content than a large number of small drops. When both large and small drops are present, the MVD is a more meaningful indicator of size distribution than the mean since it is more sensitive to presence of large drops. Mean and median drop diameters of natural clouds are usually very close to each other. In general, natural clouds can be characterized as having a drop distribution MVD in the 10 to 30 μm range, with a 20 μm MVD as a rough average. Maximum size of individual drops rarely exceeds 80 to 100 μm.

NOZZLE SELECTION

14. Prior to the 1979-80 icing season, the HISS improvement effort concentrated on finding a suitable spray atomizer to replace the existing All-American Engineering Co. (AAE) nozzles. Existing spray characteristics did not realistically simulate a natural cloud, since drop distribution MVD values ranged from 100 to 300 μm (Reference 1), with many drops of even larger diameter present. Among numerous candidate nozzles examined, the Sonic Development Corporation "Sonicore" type 125-H nozzle produced a cloud having the proper range of MVD, and generated relatively few drops larger than 100 μm. Quantitative nozzle characteristics from the icing wind tunnel evaluation are reported in Reference 2. Water flow capacity of the Sonicore nozzles is approximately 1/3 that of the AAE nozzle, requiring installation of a greater number to produce the same total LWC. Minimum air pressure for effective atomization is approximately 20 psig. As with all nozzles, spray characteristics deteriorate and unacceptably large drops appear when water pressure needed to increase flow rate approaches the air pressure value.

15. The wind tunnel results indicated that spray ejection perpendicular to the airstream produced the best results for the existing boom, and this nozzle orientation was retained from previous years. Adjacent nozzles on the boom were spaced at 6-inch intervals, alternating between top and bottom placement. Vertical distance

between adjacent nozzle ports was 11 inches. An occasional gap resulted when a nozzle location was used for boom instrumentation, or where a nozzle was removed to prevent spray impingement on the boom uplock latches.

HISS CONFIGURATION AND OPERATION

16. Two HISS configurations were evaluated using Sonicore nozzles. Initially 160 nozzles were installed, filling all available center section locations and the inboard three quarters of each outrigger. After three flights in this configuration, the nozzles were removed from the outriggers, leaving 97 nozzles installed in the center sections only. The outriggers were isolated from the boom air and water supply by metal plates bolted between the boom flanges at the outrigger junctions. The remainder of the flights used this arrangement. Measured boom air and water pressure for both configurations are shown in Figure 1, Appendix E. With 160 nozzles, the boom air pressure of 10 psig was less than the minimum needed for satisfactory water atomization. Reducing the number of nozzles to 97 increased air pressure to a nominal 20 psig which was acceptable. The pressure difference is attributed to the resulting change in total air orifice area. Comparison of the operating air and water pressure for the final configuration shows that water pressure begins to exceed air pressure beyond a 30 gallon per minute (gal/min) water flow rate, resulting in an upper usable limit of about 25 gal/min to retain satisfactory spray atomization.

17. Several other characteristics of the new system were observed during operation. Flow blockage from residual water freezing in the nozzles was greatly reduced by routing bleed air through both the air and water lines from takeoff until actual start of water flow. This proved effective to temperatures as low as -20°C, provided all residual water had first been eliminated from the boom. Occasional problems persisted, since hardware design prevented thoroughly draining all residual water prior to flight. Any future boom redesign should permit draining of all air and water lines when stowed.

18. The recorded air and water temperature changed with position on the boom, ambient temperature, flow rate, and length of spray time. Boom temperatures were generally higher after the outriggers had been blocked off, and ranged from 15° to 30° C above ambient. Icing operations at -20° C resulted in near freezing temperatures at certain boom locations, and presented a potential for freezing and flow blockage if bleed air or water flow were interrupted.

19. One of the questions concerning use of the new configuration was whether ice formations ("popsicles") would form on the boom as in previous configurations. In these tests, most ice accretion on the spray boom resulted from leakage of loose fittings between nozzles and water manifolds, and from spray impingement on the two uplock latches that hold the boom in place when stowed. Leakage was eliminated by tightening the fittings and removal of the two nozzles impinging on the uplocks. Some ice accretion developed around nozzles when flow blockage was experienced, but this was not a regular occurrence in normal operation. For practical purposes, formation of ice on the boom has been eliminated as a significant concern.

20. Partial blockage of some nozzles occurred on one flight when debris from the water tank entered the boom system. A 70 gal/min capacity in-line water filter with 100 μm elements was added and successfully eliminated this problem. One interesting development occurred during initial use of the filter. Flowing engine

bleed air through the water lines (purge air) prior to start of spray resulted in freezing and ice formation inside some nozzles. However, these nozzles were blocked by normal white ice, not the dyed yellow ice characteristic of the HISS. Hot air flow through the moist filter elements while purging had vaporized some of their contained water, which then recondensed and froze at the nozzles. Rerouting the purge air line to bypass the filter prevented nozzle freezing.

21. Evidence of uneven flow rate between the upper and lower boom sections was apparent when operating at low water flow. Downward flow routing from common sources and a difference in static head pressure due to 5 ft vertical separation resulted in a visibly thicker spray from the lower boom. At extremely low flows, spray from the upper boom would be intermittent and start to sputter. Methods to equalize water flow between the upper and lower booms should be investigated.

22. Installation of the Sonicore nozzles and adapters increased the weight of the 1634 lb boom assembly by approximately 91 lbs with 160 nozzles, or 55 lbs with 97 nozzles. Interaction between the suspended boom assembly and aircraft dynamics in flight has always existed. The added weight and drag characteristics of the new nozzles noticeably aggravated boom dynamics and increased sensitivity to turbulence. The extent of change from previous dynamics and its effect on the boom system has been investigated as part of USAAEFA Project No. 80-04 (Reference 8), and found to be acceptable.

SPRAY CLOUD DIMENSIONS

23. Size and dispersion of the spray plume depends largely on boom geometry. Using just the center boom sections (without outriggers), the spray originated from two rows of nozzles each 25 ft long, one placed 5 ft above the other. In forward flight the spray enters the atmosphere, the booms move away from that point in space and the ejected drop cloud is left behind in free air. The upper and lower plumes spread outward, undergo some turbulent mixing from residual boom vortices, merge, and finally encounter the downwash flow field and rollup from the HISS rotor wake.

24. Since the test aircraft flies a fixed distance behind the booms, it continuously encounters a new cross-section of the spreading plume. Behind the boom, the upper and lower plumes have merged by 150 ft and are entrained in the HISS downwash beyond 300 ft. The cloud edges mix with ambient air and billow from any turbulence; the entire cloud appears to "snake" behind the HISS in presence of gusts. The dynamic nature of the cloud section being swept by the test aircraft makes precise measurement of its dimensions impossible, but in-flight observation and photo comparison with known test aircraft dimensions within the cloud provides an estimate. Average cross-sectional dimensions of the present spray cloud are estimated as 36 ft wide and 8 ft deep.

25. The 8-ft depth of the present spray cloud compares to an estimated 10 to 12 ft depth in previous years using AAE nozzles. The reduced cloud depth is a result of smaller drop size, since the ejected spray could no longer penetrate into the airstream as far at right angles. With the AAE nozzles, inertial sorting by drop size generated a visible "rooster tail" effect extending outward as far as 4 ft, whereby drops would penetrate the airstream to different depths depending on their size.

26. The present cloud depth presents some limitations to comprehensive evaluation of the entire test aircraft. The 8 ft depth compares to vertical aircraft dimensions (top of hub to fuselage belly) of 11 ft (UH-1 and UH-60), and 17.4 ft (CH-47). As the spray cloud reaches the test aircraft, it is also deflected downward by rotor downwash. Dividing immersion in phases between rotor and fuselage provides a partial solution. Even so, vertical separation between components such as ice detectors and the systems they protect presents difficulty in simultaneous exposure to a uniform icing environment.

27. Without spray from the outriggers the estimated width of the cloud was 36 ft. While less than any test aircraft rotor diameter, full span ice accretion was demonstrated on all rotor systems, including the 60-ft diameter of the CH-47D. Since each part of the blade passes through the plume at least once every revolution, the main question centers on definition of the applicable spanwise LWC. Inboard blade portions are always within the plume, while the outer portions experience less exposure.

28. Use of the outriggers extends cloud width from the upper boom and permits more leeway for lateral motion of the test aircraft. However, the outrigger spray pattern at the test aircraft is less uniform than from the center sections. Spray from the center sections does not merge laterally with that from the outriggers. Two vertical boom sections suspend the spray assembly and attach between the horizontal center sections and outriggers. Across these junctions a gap of 20 inches separates adjacent nozzles on the top bar, compared to 6 inches elsewhere. These spaces, and the airflow characteristics around the junction flanges, creates two gaps in the cloud, each 6 to 7 feet wide at the test aircraft. With a UH-1 (48-ft rotor diameter) centered in the cloud, spray from even the inner portions of the outriggers remains outside the rotor disk. This phenomenon was less noticeable in the past because of the previous lateral nonuniformity of the cloud caused by the wide AAE nozzle spacing.

29. Another factor affecting spray from the outriggers is its entrainment in the HISS rotor wake. This roll-up disturbs spray from the outboard portions as early as 100 ft behind the spray boom, or less than half the distance for the center sections. Much of the spray from the outriggers diverges outward to such an extent that it never reaches the test area. Using the outriggers in their present configuration does not produce a uniform cloud cross-section because of both the large gaps generated by the vertical supports, and the roll up divergence of spray from the outboard sections of each outrigger.

MRI DATA ANALYSIS

30. The MRI particle measuring probes generate a continuous stream of 1-second samples. Each sample contains a drop number count and classifies drop diameter into 15 separate channels per probe. All measured cloud parameters are derived from the drop number count, diameter classification, and size of the air volume sampled. Sample volume size depends on airspeed and the type of probe. Measurement accuracy for any given drop is limited by the resolution of the size class it falls within. Of the three probes, the ASP (3 to 45 μm total range) has the narrowest channels, each 3 μm wide. A measured drop is assumed to lie in the center of its size class, although its actual diameter may fall anywhere within the channel. To calculate LWC, the volume of water contained by individual drops is summed and related to the total volume of air sampled. The range of uncertainity in drop diameter (channel width) can produce a variation of 10 to 20% in expected accuracy for LWC.

31. While this report summarizes only the data applicable to the HISS, all the MRI data are given in Reference 7, to include natural icing conditions. MRI presents a total of 51 HISS cloud measurements taken during 5 flights as spectral format data listings. These points represent stable conditions with the probes centered in the spray cloud and are summarized in Table 2 as to ambient conditions, flow rate, and measured cloud characteristics. While each condition was held constant for as long as 2 minutes, these points are actually single 1-second samples selected by MRI to represent the average condition for each case. A capability exists to average the spectral data over longer time segments, and this should be used in future programs to minimize possible bias.

32. In addition to the 51 steady-state measurements, MRI analyzed a number of vertical and horizontal sweeps through the cloud. To define spatial variation of LWC and MVD, the data samples taken during these sweeps were analyzed point by point and correlated against time with estimated position in the cloud. MRI provides summary plots for these in Reference 7, but does not include spectral format printouts for the specific points used.

33. A number of flights resulted in data that were not used for the final MRI analysis. These included the first several flights in the initial configuration (low boom air pressure), flights for IPS checkout of the measurement aircraft (probes not immersed in cloud), and flights that experienced nozzle flow difficulty and blockage by freezing (non-uniform cloud). One problem affecting the MRI ASP measurements persisted throughout the program, and is described in more detail in Reference 7. Electrical noise peculiar to the 400Hz aircraft power supply and probe electronics package disabled the ASP velocity rejection circuitry, affecting the logic used to compensate for known errors when counting drops that pass through the fringes of the sample volume. This resulted in measurement of much higher values of LWC than actually present. Determination of the problem was not accomplished until near the end of the flight program, requiring subsequent correction and reprocessing all available ASP data. The last flight of the program (No. 27) used a new ASP probe and was not subject to the error. However, this flight took place in turbulent atmospheric conditions, and quality of the resulting data was suspect. MRI does not present spectral data listings from this flight in Reference 7. The following paragraphs present an analysis of the MRI cloud data with respect to LWC, MVD, and drop size distribution for the current HISS.

LIQUID WATER CONTENT

34. If the spray cloud were homogeneous, LWC would be uniform at a constant value throughout the cloud. Such a value can be calculated from the known water flow rate, airspeed, and cloud cross sectional area, by the expression:

$$\mathrm{LWC} = \frac{1320.06 \times \text{flow rate}}{\text{airspeed} \times \text{area}}$$

where: LWC = gm/m^3
flow rate = gallons/minute
airspeed = KTAS
cross sectional cloud area = ft^2
1320.06 = conversion factor for units shown

This function assumes no loss of liquid water through evaporation. It is useful in providing a calculated average for LWC over the entire cloud cross-sectional area. For a fixed airspeed and cloud size, LWC is a linear function of flow rate.

Table 2
HISS Cloud Measurements[1]

Flight No.[2] and Average Ambient Conditions	Point Identifier (sample time)	Standoff Distance (ft)	Water Flow Rate (gal/min)	MEASURED SPRAY CHARACTERISTICS[3]			
				Liquid Water Content (gm/m^3)	Drop Number Concentration (No./cm^3)	Median Volumetric Diameter (μm)	Mean Volumetric Diameter (μm)
Flt 8	12:29:29	150	30	1.36	281	34	20.9
	12:37:47	150	19	1.18	375	28	18.2
T = -13°C	12:43:58	150	14	.89	338	26	17.1
H_p = 1800 ft	12:50:21	150	9	.58	208	27	17.5
RH = 63%	13:04:00	150	40	1.29	166	73	24.6
	13:10:15	150	35	.62	33	79	32.5
	13:16:52	150	25	1.08	264	32	19.8
Flt 9	11:06:55	200	19	1.15	243	46	20.8
	11:09:00	300	19	1.33	224	65	23.0
T = -11°C	11:12:50	200	14	.84	451	27	15.2
H_p = 1800 ft	11:15:35	300	14	.90	405	27	16.2
RH = 85%	11:19:06	200	11	.74	462	23	14.6
	11:22:15	300	11	.87	480	24	15.1
	11:25:18	200	9	.66	515	21	13.5
	11:28:55	300	9	.67	358	24	15.2
	11:32:12	200	6	.35	340	23	8.9
	11:36:19	300	6	.44	358	22	13.3
	11:39:52	200	4	.38	364	19	12.6
	11:42:50	300	4	.42	306	20	13.6
	11:46:03	200	30	1.33	459	63	17.6
	11:52:03	200	50	2.03	518	107	19.5
	11:54:57	200	25	.81	99	94	24.8
	12:01:54	200	7	.27	72	74	19.3
Flt 10	13:43:53	150	14	.89	282	37	17.8
	13:45:27	150	11	.75	490	24	14.3
T = -9.5°C	13:48:10	150	9	.61	474	22	13.5
H_p = 3000 ft	13:51:01	150	8	.52	488	21	12.2
RH = 75%	13:53:12	150	7	.56	477	23	13.1
	13:55:27	150	6	.48	418	21	13.0
	13:57:45	150	5	.29	310	20	12.2
	14:00:09	150	4	.38	379	21	12.4
	14:14:38	150	14	.84	314	33	15.2
	14:17:09	150	11	.70	299	30	16.5
T = -17°C	14:19:36	150	9	.64	291	29	16.2
H_p = 10,000 ft	14:21:58	150	8	.49	282	25	14.9
RH = 75%	14:23:53	150	7	.55	329	24	14.7
	14:25:55	150	6	.53	355	24	14.2
	14:27:45	150	5	.37	218	25	14.8
	14:31:03	150	4	.45	271	32	14.7
Flt 12							
	09:57:01	150	11	.71	443	24	14.5
T = -10°C	09:51:52	150	13	.87	496	24	15.0
H_p = 2500 ft	09:47:53	150	15	.93	378	30	16.7
RH = 85%							
Flt 13	08:44:52	150	4	.34	445	19	11.4
	08:48:43	150	5	.42	421	21	12.4
T = -9.5°C	08:50:42	150	6	.52	472	21	12.8
H_p = 2900 ft	08:54:40	150	7	.55	434	22	13.4
RH = 85%	08:57:32	150	8	.52	400	21	13.6
	09:00:56	150	9	.59	377	22	14.4
	09:03:24	150	11	.69	470	22	14.1
	09:06:46	150	13	.82	499	23	14.6
	09:09:47	150	15	.96	448	27	15.8

[1] Data taken at 90 KTAS during stable immersions centered in the spray cloud.

[2] HISS configuration: 97 Somecore nozzles installed on the spray boom center sections only.

[3] Measurements made with an Axially Scattering Probe and a Cloud Particle Spectrometer furnished by MRI.

35. Measured values of LWC for the steady state "cloud centered" points of Table 2 are shown as a function of flow rate in Figure 2. This figure also includes data from a different ASP probe (flight No. 27) which do not appear in Table 2. For comparison, also shown is the calculated average line derived for an 8 x 36 ft cloud cross section area (288 ft^2) at 90 KTAS.

36. The range of observed scatter in measured LWC can be explained by non-uniform distribution of water within the spray cloud, as was measured during the vertical sweeps. Variation of LWC with vertical position in the cloud is summarized in Figure 3 for three water flow rates (4, 9, and 14 gal/min). In producing a fairing for each flow rate the number of vertical sweep data points used were 41, 49, and 39 respectively, representing a collection of data from several flights. LWC scatter for the selected points used was generally within ±0.2 gm/m^3 of the faired lines, providing a reasonable degree of confidence in the trends shown.

37. The approximations consistently show maximum LWC somewhat below cloud center, and decreasing LWC toward both the top and bottom of the cloud. Since some vertical movement of the aircraft is inevitable while immersed in the cloud, the anticipated range of LWC variation suggested by these trends is of interest. Table 3 presents alternate LWC values for various portions of the cloud, derived from the faired curves of Figure 3. Integrating the area bounded by these curves yields LWC over any given vertical segment of the cloud. The "integrated average" represents LWC taken over the cloud as a whole (from top to bottom), while the "maximum" is the single highest LWC value occuring at the knee, somewhat below cloud center. The other values represent LWC within five vertical portions of the cloud: top 2 ft, center to 2 ft above, center to 2ft below, the central 4 ft segment (center ± 2 ft), and bottom 2 ft. The "maximum", "integrated average", and central segment measurements are shown graphically in Figure 4, which also shows the calculated average function for comparison. The "center - 2 ft" cloud section LWC is close to the "maximum" curve, while the "center + 2 ft" LWC approximates the "integrated average" curve. The average taken from "center ±2 ft" of the cloud lies between these extremes. A discrepancy occurs where the "integrated average" over the entire cloud exceeds the calculated average for the 4 gal/min flow rate: this implies more water being measured in the air than was pumped from the spray booms. The size of this discrepancy is not large, and can be attributed to data inaccuracy deriving from (a) the inherent 10 to 20 percent uncertainty in the LWC measurement technique, (b) the 1-gal/min resolution of the flowmeter used to adjust HISS water flow.

Table 3. Values of Liquid Water Content (gm/m^3)
Contained in Various Regions of the HISS Spray Cloud

Region of Cloud	Water Flow Rate ~ gal/min		
	4	9	14
Integrated Avg	.29	.42	.56
Maximum	.52	.69	.91
Top 2 ft	.10	.14	.17
Ctr + 2 ft	.28	.44	.57
Ctr ± 2 ft	.38	.55	.72
Ctr - 2 ft	.48	.66	.86
Bottom 2 ft	.33	.43	.64

[1] HISS configuration: 97 Sonicore nozzles installed on the spray boom center sections only.
[2] LWC calculated by integrating vertical water distribution profiles over defined horizontal layers.
[3] Average water distribution profiles based on a collection of vertical sweep data from several flights.
[4] Data taken at 90 KTAS.

38. In practical terms, aircraft components that vary location within ±2 ft of cloud center will experience LWC exposure that ranges between the maximum value measured and the "integrated average". Comparison of these curves with the range of Figure 2 data for the steady state "cloud centered" measurements shows that most of these points fall within the cloud "center ± 2 ft" boundaries. As could be expected, these values are generally higher than the calculated average LWC, since the LWC profiles contain less water in the outer fringes of the cloud. A test aircraft rotor system will pass through all portions of the spray cloud, and some segments will be outside the cloud part of the time. For a desired LWC, the calculated average line should be used to determine required water flow rate when humidity is high and evaporation can be neglected.

39. Points from the last flight (No. 27) taken with the new ASP generally fall below the rest of the Figure 2 data, but are suspect because of turbulent flight conditions. Data at higher than 25 gal/min flow rates also fall below expected LWC values, and this is attributed to a breakdown in nozzle atomization. This produces large diameter drops which contain significant LWC but do not always get measured by the MRI probes.

40. MRI also analyzed LWC data from horizontal sweeps through the cloud. The data show a relatively constant LWC across the central portion of the cloud, tapering to zero at the edges. This transition area of reducing LWC includes approximately one-quarter width of the cloud (9 ft) at each edge. In the central region, LWC is much more sensitive to vertical rather than horizontal position.

CLOUD DROP MEDIAN VOLUMETRIC DIAMETER

41. The MRI analysis of cloud drop MVD also used vertical sweep data from several flights., and is summarized in Figure 5. While MRI did not give spectral data listings for the specific points used, the MVD size range was generally within 20 to 40 μm, except within the lower quarter of the cloud (bottom 2 ft) where MVD values as high as 70 μm were seen. Figure 5 compares cloud MVD as produced by the current Sonicore nozzles with measurements of the spray produced by the AAE nozzles during previous HISS icing tests (Reference 1). The current HISS cloud MVD represents a vast improvement over the artificial cloud of previous years, and overlaps the 10 to 30 μm MVD range representative of natural icing clouds.

42. MRI analysis of the vertical sweep measurements gave higher values of MVD (up to 70 μm) in the bottom 2 ft of the cloud. This increase was primarily observed at very low flow rates, and was caused by an absence of small drops, not by an increase in the number of large drops. The reasons for this shift to larger MVD in the lower part of the cloud are not clear, but are probably related to gravitational sorting by size, buoyancy effects for small drops, and flow rate differences between the upper and lower spray booms.

43. Figure 6 shows cloud MVD as a function of water flow rate for the steady state "cloud centered" [illegible] in Table 2. A high concentration of this MVD data falls between 20 and 35 μm. However, increasing MVD size and added scatter are seen above water flow rates of 19 gal/min. In this range, nozzle performance is very sensitive to small changes in applied air and water pressure. When the pressures are close to each other, and especially when water pressure exceeds air pressure, atomization deteriorates and large drops are produced. An example can be seen

in the 4 consecutive points taken from Flight 9: water flow was increased from 30 to 50 gal/min, causing a breakdown in atomization. Subsequent reduction of flow to 7 gal/min failed to restore proper nozzle performance, and the MVD remained high even at the lowered flow rate.

44. Actual MVD values at high water flow are probably somewhat larger than the 60 to 110 μm values shown in Figure 6. The measured LWC for these flow rates is less than expected from mass conservation: this implies that the missing water content consists of fairly large drops not seen by the probes. If these large drops were included in the measured spectrum, MVD would then be driven upward considerably. To retain proper atomization while operating at higher values of water flow (i.e. to remain within the recommended performance envelope of the nozzle), air pressure must be increased beyond levels presently available on the HISS. Ways to supplement pressure and flow rate of the engine bleed air source should be investigated.

45. The distinction between median (MVD) and mean drop diameter can be seen in Table 2. Values of MVD are sensitive to large drops, and range between 19 and 107 μm, while mean diameters generally fall into a narrow band from 12 to 18 μm. Extreme values of mean diameter vary from a low of 9 to a high of 32 μm, and fail to indicate the relative quality of drop size distribution within the spray. Mean drop diameters of the spray plume in previous years have clustered around 50 μm, while MVD varied from 100 to 300 μm.

CLOUD DROP DISTRIBUTION

46. The MRI spectral format listings in Reference 7 give actual drop distribution data for each of the steady state "cloud centered" points of Table 2. Each listing combines data from both probes on the measurement aircraft into 28 size classes, ranging from 3 to 300 μm. The drop number count and mass (LWC) in each channel are shown, both as normalized values (per cubic meter) as well as per unit channel width (per cubic meter per μm channel width). Incremental and cumulative percentages of total LWC are also given.

47. The MRI plot formats used to illustrate cloud composition show drop number concentration and mass distribution vs drop diameter. Both types of plot present the same data in different formats: one shows the number of drops in each size range, while the other shows the mass (LWC) contained in each range (density of water is assumed constant at 1 gm/m^3). Figures 7 and 8 compare a typical HISS cloud measurement in the present configuration with data from 1978-79 (Reference 1) for both the HISS spray plume and a natural cloud. The drop size improvement in HISS cloud composition over past years represents two orders of magnitude in number concentration (Figure 7) and one order of magnitude in mass distribution (Figure 8). While the present data more closely approximate a natural cloud, some differences still exist. Natural clouds have somewhat more mass in the 10 to 20 μm drop range, and the present HISS cloud still contains some drops larger than 100 μm.

48. Total drop number concentrations were generally several hundred per cubic cm, and are typical of numbers seen in natural clouds. The HISS spray cloud produced by the original AAE nozzles had considerably lower number counts of 0.5 to 4 drops/cm^3.

49. MRI presents several plots to illustrate effects on cloud composition due to variation in flow rate, standoff distance, and relative humidity. The most significant flow rate effect occurs when 25 gal/min is reached: breakdown in atomization generates a pronounced peak at 80 μm drop diameter as well as a considerable number of larger drops. The effects of standoff distance and humidity are primarily a result of drop evaporation: lower humidity allows quicker evaporation, and greater distance provides more time for evaporation to take place. Evaporation primarily reduces the amount of water contained in drops smaller than 20 μm.

50. Relative humidity is the most pronounced difference between a natural icing cloud and the artificial test environment in clear air. A natural cloud is saturated with a background relative humidity of 100%. This water in vapor form exists in addition to any LWC as liquid drops. The vapor alone represents about 5 gm/m^3 at 0° C, and 1 gm/m^3 at -20° C. The high relative humidities encountered during this test program (lowest value of 63%) did not provide sufficient data for extensive analysis of evaporative effects on the spray cloud. Since the reduction in drop size over previous years places a substantial amount of LWC in the small size range below 20 μm most affected by evaporation, future programs using the HISS should place greater emphasis on investigation of evaporative effects.

ICE ACCRETION ON TEST AIRCRAFT

51. In addition to the cloud measurements and ice phobics evaluation performed by the UH-1H, other icing projects also accumulated immersion time in the HISS spray cloud: 5.6 hrs during 7 flights with a CH-47D (USAAEFA Project 79-07), and 3.7 hrs during 4 flights with a UH-60A (USAAEFA Project 79-19). These aircraft also flew numerous evaluations in natural icing during the same test period, and their concurrent exposure to artificial icing allowed comparison between icing characteristics of both environments.

52. Test aircraft ice formations produced with the artificial cloud compared favorably with those seen in the natural environment. Both location and appearance of accreted ice resembled that typically seen on natural icing flights. Previously HISS ice formations tended to be massive and relatively clear, covering any exposed frontal area in a thick layer. In the present configuration, this type of ice was only seen at the high flow rates, where the nozzles were no longer atomizing properly and tended to produce large drops. In normal operation, various swept surfaces of the test aircraft would accrete a scalloped ice formation similar to that seen in natural conditions.

53. Comparison of past and present ice formations produced by the HISS gave several indications of a smaller and more realistic drop size distribution. Artificial ice was now appearing on UH-1H inlets, a condition common in the natural environment but not previously duplicated behind the HISS. Small drops are able to make the 90° turn and collect on the inlets while large drops with greater inertia fail to turn and miss the inlet. Ice also formed on individual rivets of the UH-60A and UH-1H tailbooms; this type of small discontinuity on a smooth surface collects ice in a natural cloud, but had not been previously observed with the HISS. Another indication was the type of ice formed on the UH-60A droop stops and flap restrainers. Icing of these components prevented their engagement during shutdown

both in natural and artificial conditions. Previous artificial testing had failed to identify the problem, since ice had not formed on these components in this way with the spray cloud then available.

CONCLUSIONS

GENERAL

54. The following conclusions were reached upon completion of the in-flight HISS nozzle evaluation.

a. Nozzle water pressure begins to exceed air pressure beyond a 30 gallon per minute water flow rate, resulting in an upper usable limit of about 25 gal/min to retain satisfactory spray atomization (Para 16).

b. Average cross sectional dimensions of the present spray cloud are estimated as 36 ft wide and 8 ft deep (Para 24).

c. The current HISS cloud MVD represents a vast improvement over the artificial cloud of previous years, and overlaps the 10 to 30 μm MVD range representative of natural icing clouds (Para 41).

d. The drop size improvement in HISS cloud composition over past years represents two orders of magnitude in number concentration and one order of magnitude in mass distribution (Para 47).

e. Test aircraft ice formations produced with the artificial cloud compared favorably with those seen in the natural environment (Para 52).

RECOMMENDATIONS

55. The following recommendations are made:

a. Any future boom redesign should permit draining all air and water lines when stowed (Para 17).

b. Methods to equalize water flow between the upper and lower booms should be investigated (Para 21).

c. The MRI capability to average cloud spectral data over longer time segments should be used in future programs (Para 31).

d. For a desired LWC the calculated average line should be used to determine required water flow rate when humidity is high and evaporation can be neglected (Para 38).

e. Ways to supplement pressure and flow rate of the engine bleed air source should be investigated (Para 50).

f. Future programs using the HISS should place greater emphasis on investigation of evaporative effects (Para 50).

APPENDIX A. REFERENCES

1. Final Report, USAAEFA Project 78-21-2, *Microphysical Properties of Artificial and Natural Clouds and their Effects on UH-1H Helicopter Icing*, August 1979.

2. Final Report, Boeing Vertol Company No. D210-11570-1, *Helicopter Icing Spray System (HISS) Improvement Program*, February 1980.

3. Paper, American Helicopter Society, 36th Annual Forum, Preprint No. 80-63, *Helicopter Icing Spray System*, May 1980.

4. Letter, AVRADCOM DRDAV-DI, 9 Nov 1979, Subject: *HISS Improvement and JUH-1H Ice Phobic Coating Natural and Artificial Icing Tests, Revision 2*, AVRADCOM Test Request, Project No. 79-02.

5. Test Plan USAAEFA Project No. 79-02, *HISS Improvement JUH-1H Ice Phobic Coating Natural and Artificial Icing Tests*, November 1979.

6. Final Report, USAAEFA Project 79-02, *JUH-1H Ice Phobic Coating Icing Tests*, July 1980.

7. Report, Meteorology Research, Inc., No. MRI 80 FR-1748, *Droplet Size and Liquid Water Characteristics of the USAAEFA (CH-47) Helicopter Spray System and Natural Clouds as sampled by a JUH-1H Helicopter*, August 1980.

8. Final Report, USAAEFA Project 80-04, *Helicopter Icing Spray System Evaluation and Improvements*, June 1981.

9. Handbook, All American Engineering Co. SM-280A, *Installation, Operation, & Maintenance Instructions with List of Parts, Helicopter Icing Spray System (HISS)* with change 1, November 1974.

APPENDIX B. DESCRIPTION

1. The Helicopter Icing Spray System (HISS) was manufactured by the All American Engineering Co. (AAE) in 1972 for installation in a modified CH-47C helicopter. The original system was modified to its present configuration in 1975, and a detailed description of its components appears in the AAE Handbook of installation, operation, and maintenance instructions (Reference 9, Appendix A). Additional modifications resulted from the nozzle improvement evaluation described in this report.

2. The HISS is installed in CH-47C S/N 68-15814, and consists of an internal water tank and an external spray boom assembly suspended 19 ft beneath the aircraft from a cross-tube through the cargo compartment, as shown in figure 1. Hydraulic actuators rotate the cross-tube to raise and lower the boom assembly within 30 to 45 seconds. The spray booms are held in the down position by two locking struts or held in the stowed position by two fuselage-mounted latches. The water tank is mounted in a cradle and has an 1800 gallon capacity, but weight and center-of gravity limitations for flight restrict filling it beyond 1400 gallons. A cable-cutter assembly allows emergency jettison of the internal water supply through doors in the base of the tank above the fuselage opening at the aircraft cargo hook location. The external boom assembly can also be jettisoned by actuating explosive bolts installed in a joint on each of the boom support arms.

3. A calibrated air temperature probe and a Cambridge dew point hygrometer provide accurate ambient temperature and humidity measurement. An aft-facing radar altimeter is mounted at the rear of the HISS to allow positioning the test aircraft at a known standoff distance. The HISS aircraft is limited to a takeoff gross weight of 46000 lbs. The aft fuel tanks are left empty and 806 gallons of fuel can be carried in the main and forward auxiliary tanks. Normal operating main rotor speed is 245 RPM, but below 40000 lbs, 235 RPM may be used. Rotor speed is kept constant at the selected RPM during spray operation. A density altitude limit of 12000 ft is imposed, but normal operations do not exceed 10000 ft pressure altitude. Test flights are conducted at any selected altitude between this height and 1500 ft above ground level, as chosen for a desired ambient temperature. Airspeed limitations vary as a function of gross weight and density altitude. Flight conditions are controlled to not exceed limits shown on a cruise guide indicator that measures stress loads imposed on the pivoting actuator and the fixed link of the aft rotor flight control system. USAAEFA project no. 80-04 (Reference 8, Appendix A) found stresses of the spray boom in its present configuration to be satisfactory at airspeeds to 140 KTAS. While raising or lowering the boom assembly, airspeed is held to 40 KTAS.

4. Water flow to the spray booms is controlled by manual water line valves and a hydraulic pump valve. A shutoff valve isolates the water tank from the pump. A hydraulic control valve regulates the hydraulically operated water pump motor, which is capable of flow rates in excess of 140 gal/min. A pressure gage indicates water pressure at the pump outlet. An in-line volumetric turbine flowmeter is installed downstream of the pump. A pulse rate integrator supplies the necessary signals to drive both an analog dial gage and a digital panel meter showing water flow rate. The digital panel meter has a resolution of 1 gal/min and is used by the crew to adjust the desired flow rate. The dial gage also contains a digital counter to show gallons of water consumed. Water remaining in the tank can also be read on two plastic sight gage tubes installed along the tank. Two additional valves are installed

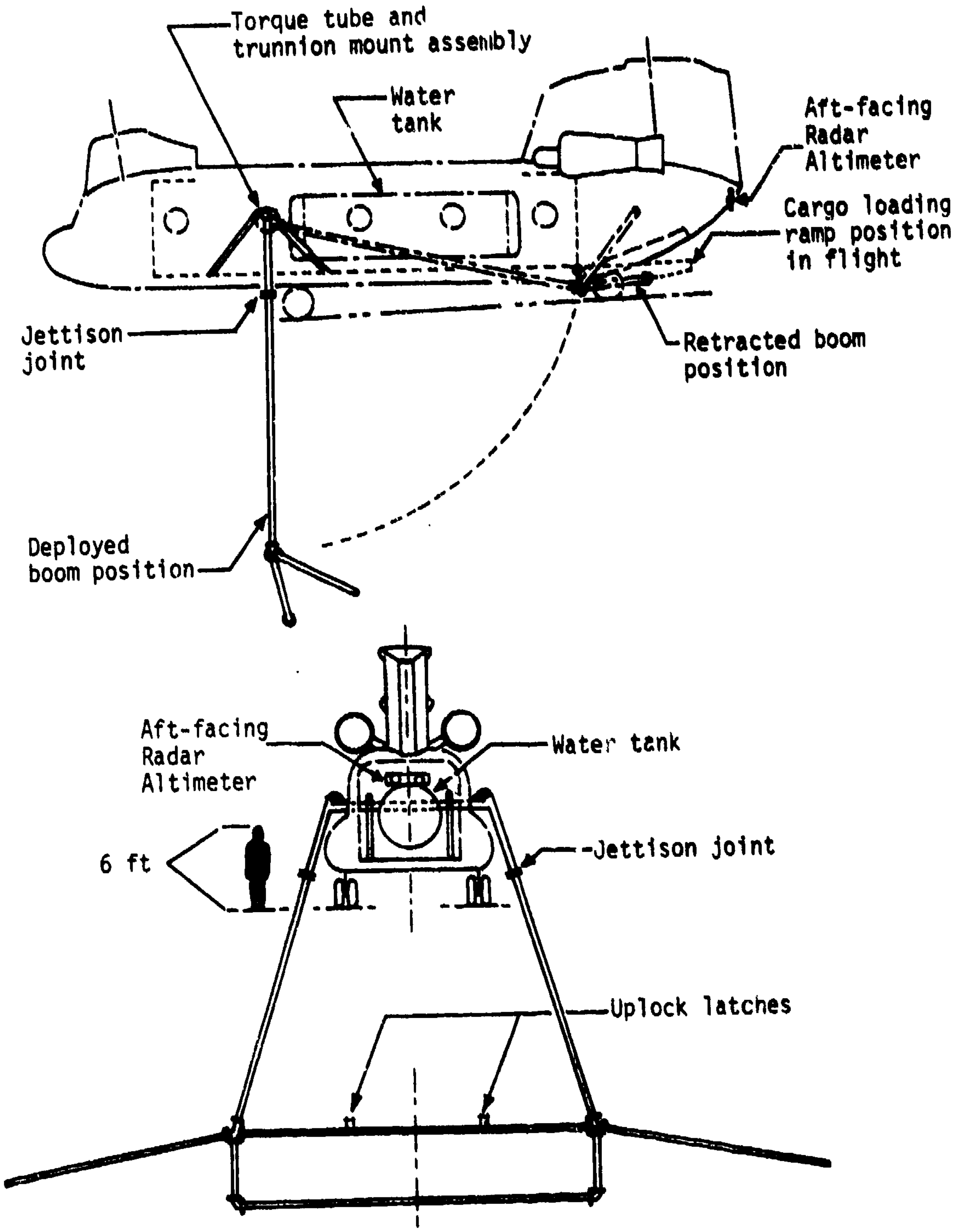

Figure 1. Helicopter Icing Spray System Side and Rear View Schematics

downstream of the flowmeter, where the water line splits into two parallel pipe diameters to allow control at high and low flow rates. Below 25 gal/min, only the small valve is opened, and can be throttled to adjust pump outlet pressure in combination with the upstream hydraulic control valve. The water pipes rejoin to flow through the 70 gal/min capacity water filter containing 100 μm elements installed during this project. From here, the water flow is split by a Y-junction and enters the torque tube assembly to flow down the boom supports on each side of the aircraft to the spray boom assembly. An additional valve downstream of the water filter allows flow of engine bleed air through the boom water lines to purge any remaining water once spray operations are concluded.

5. Air to the boom assembly is furnished by engine compressor bleed from the aircraft Lycoming T55-L-11ASA engines. The spray boom system taps into the customer bleed air manifold through the Boeing-Vertol furnished valves that normally supply inlet D-ring anti-ice. These valves are mounted on the engine and are controlled from the cockpit. Flow is then routed into the cargo compartment where additional manual valves are installed for each engine. The flows combine into a single duct which is routed forward to the torque tube and boom supports through a regulator. The regulator contains two gages showing input and output air pressure, but was adjusted to allow unrestricted air flow. This was the original AAE configuration as used in this evaluation. Subsequent modifications to the engine mounted bleed air valves, duct routing, and elimination of the regulator were performed for USAAEFA project 80-04, and are described in Reference 8, Appendix A.

6. The spray boom consists of two 27 ft center sections, vertically separated by 5 ft, and two 17.6 ft outriggers attached to the upper boom. The outriggers are swept aft 20° and angled down 10°, giving a tip to tip boom width of 60 ft. Water and bleed air are routed downward from the aircraft to the boom assembly through the two boom supports. The boom is assembled of concentric metal tubing: the inner pipe (1-1/2" diameter) acts as the water supply and leads to 30 manifolds spaced approximately 3 ft apart along the boom exterior; the outer pipe (4" diameter) contains bleed air from the aircraft engines and is fitted with a total of 172 receptacles on the boom surface as shown in Figure 2. These nozzle receptacles are spaced at 1 ft intervals along the top and bottom of the boom and are staggered to provide alternating upward and downward ejection ports every 6 inches. Thermocouples and pressure transducers described in Appendix C were installed on the boom assembly for this evaluation to allow in-flight measurement of pressure and temperature for both boom air and water.

7. For this evaluation the original AAE atomizers that are described in Reference 9, Appendix A were removed. In their place, Sonic Development Corporation Model 125-H Sonicore nozzles were installed, as shown in Photo 1. These nozzles have a converging-diverging air orifice with a throat diameter of 0.125 inches and an exit diameter of 0.19 inches. Four 0.043 inch diameter holes are arranged inside the air channel downstream of the throat to inject water. A resonator cap assembly is centered over the exit orifice to create a standing shock wave and atomize the emerging water with sonic energy. Adapters were fabricated to fit the nozzle receptacles on the boom and attach to the base of the Sonicore nozzles with 1/8 inch NPT threaded nipples. Air enters at the base of the nozzle and water from the side. As installed on the boom, vertical distance between upward facing and downward facing nozzle orifices was 11 inches. Initially, 160 nozzles were installed on the boom center sections and outriggers, as shown in photo 2. However, the final

configuration evaluated had 97 Sonicore nozzles mounted on the two boom center sections only, as shown in photo 3.

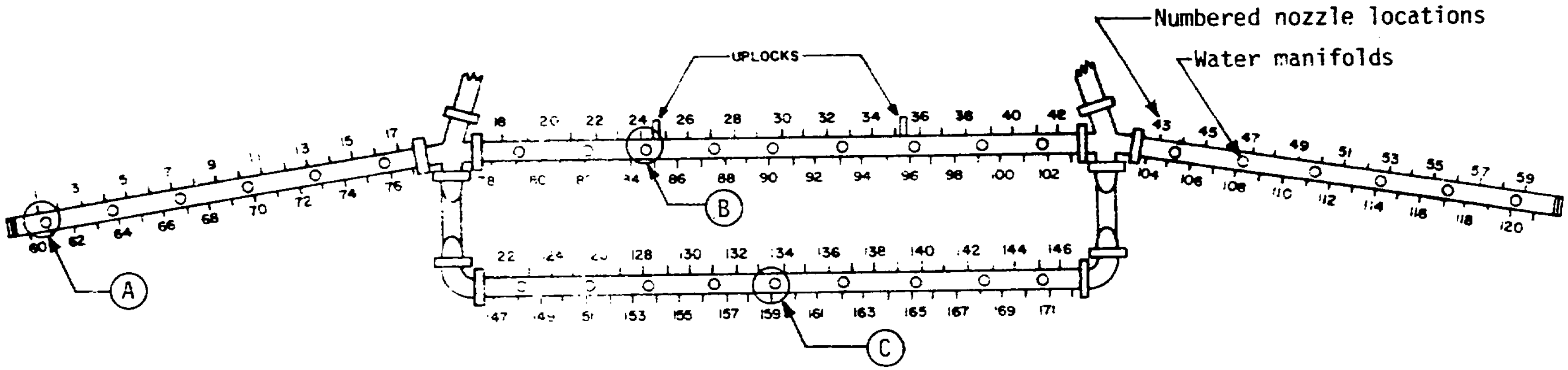

NOTES:
1. Not to scale
2. A, B, and C are locations used to install pressure and temperature sensors for boom air and water on the left outrigger and upper and lower center sections.
3. Total of 172 nozzle receptacles: 35 per each outrigger, 51 per each center section.
4. Total of 30 water manifolds: 6 per each outrigger, 9 per each center section.

Figure 2. Spray Boom Schematic Showing Locations of Nozzle Receptacles and Water Manifolds

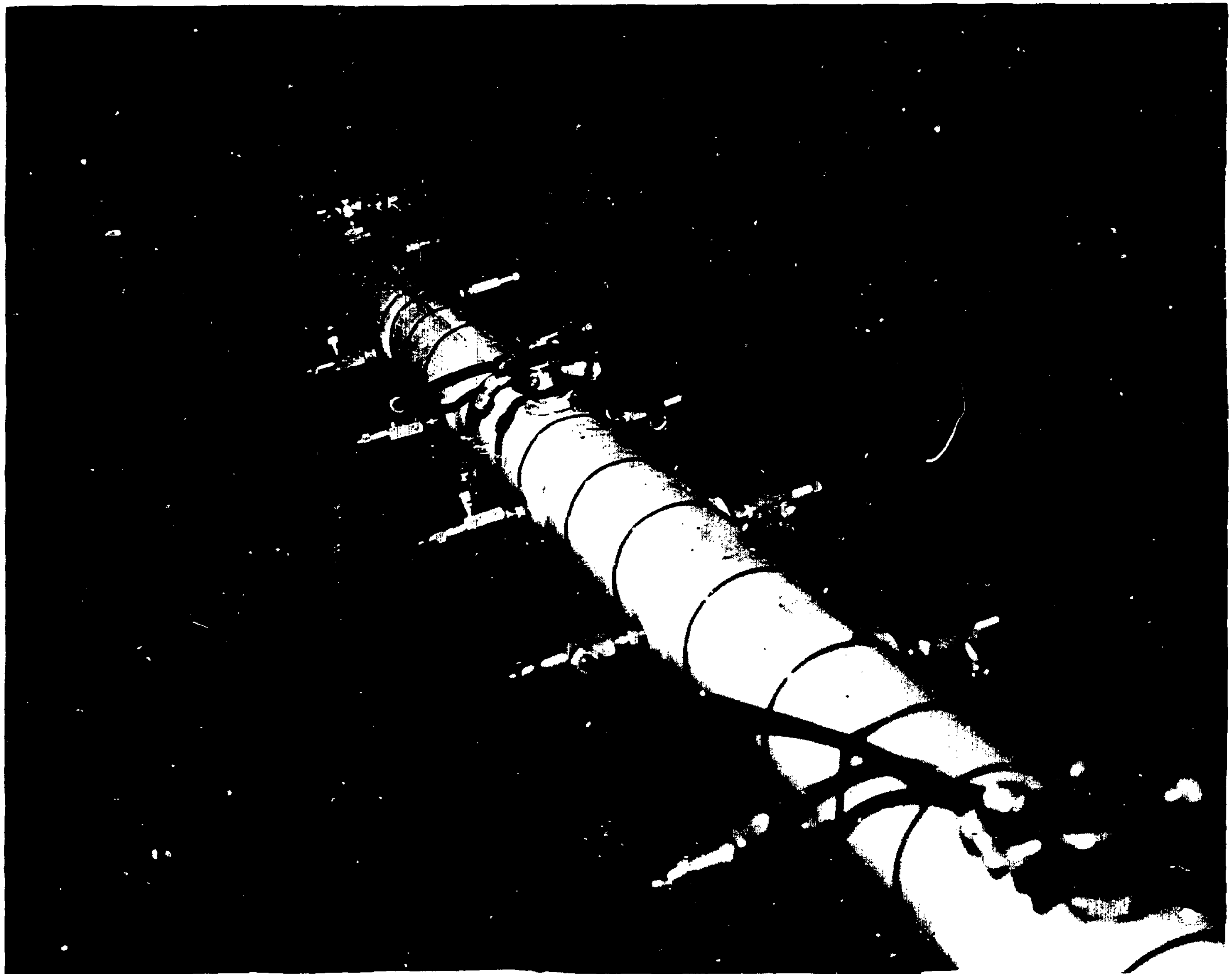

Photo 1. Sonicore Nozzles Shown Installed on Left Outrigger of Spray Boom.

Photo 2. HISS Spraying with 160 Sonicore Nozzles Installed on Spray Boom Center Sections and Outriggers (initial Configuration).

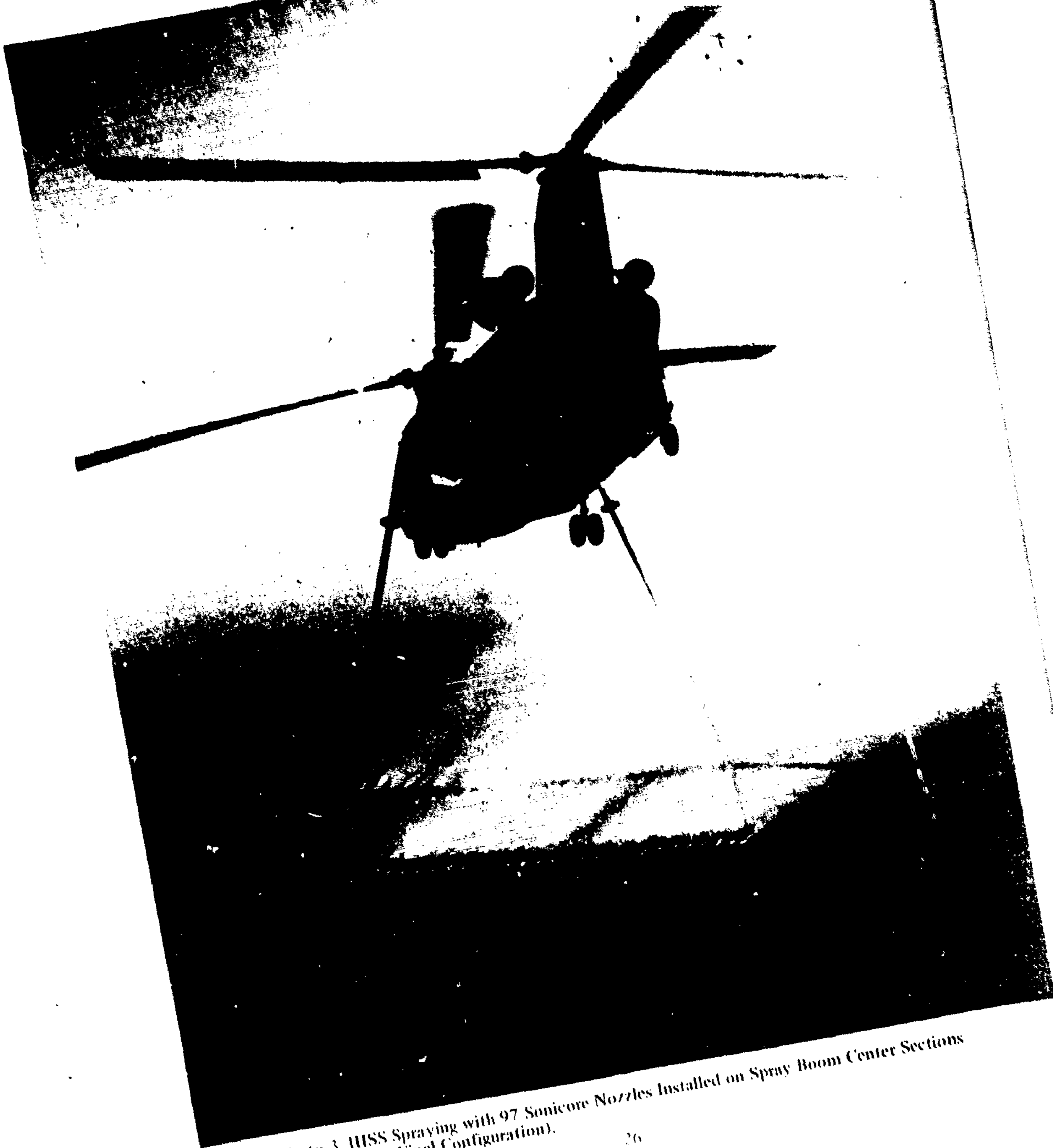

Photo 3. HSS Spraying with 97 Sonicore Nozzles Installed on Spray Boom Center Sections Only (Final Configuration).

APPENDIX C. INSTRUMENTATION

SPRAY BOOM INSTRUMENTATION

1. To obtain in-flight pressure and temperature data for both air and water within the spray boom, pressure transducers and iron-constantan thermocouple wires were installed. Three locations on the boom were used as indicated in Figure 2 of Appendix B: left outrigger tip, left uplock on the upper center boom, and middle of the lower center boom. The first two locations were used for the 160-nozzle configuration and the latter two for the 97-nozzle configuration.

2. Access to boom air (Photo 1) was gained by removing a nozzle and its adapter, and replacing it with a metal disk drilled to hold the sensor. This disc was the same type as the dummy disks normally used to seal off unused nozzle locations which fit into any nozzle receptacle on the boom surface. The sensor was exposed to the same interior boom air that would normally enter the base of the nozzle at that location.

3. Boom water was measured at the water manifolds (Photo 2) located along the boom exterior. Each manifold has 6 threaded ports to supply water through plastic tubing to nearby nozzles. Removal of one tube and its fitting allowed access to a manifold port where a threaded sensor mount could be installed. With the sensors installed, the manifold continued to supply water to 4 nozzles.

4. Wire from the thermocouples and pressure transducers was routed along the boom surface and up the left support into the HISS through the cabin window from which the boom-support torque tube extends. A control and display panel was mounted in the left side of the cabin on the avionics rack behind the cockpit (fuselage station 120). As shown in Photo 3, four separate indicators were available to display boom pressure (two air and two water), and a digital neon-tube display allowed selection of any of four temperatures (two air and two water).

5. These measurements were read and recorded manually on several flights. The transducers used for boom water pressure could not sustain repeated exposure to the changing conditions encountered (i.e. bleed air during purge alternating with cold water that sometimes froze in the manifolds during operation). As a result, boom water pressure was available only for part of the program. A gage showing water tank pump outlet pressure was also available as part of the standard HISS installation. This pressure was generally a few psig less than measured at the boom.

PARTICLE MEASURING PROBES

6. The JUH-1H measurement aircraft was equipped with an instrumentation package and recording system furnished by MRI. Three probes manufactured by Particle Measurement Systems Inc. were available for spray cloud measurement:

a. Model ASSP-100 axially scattering probe (ASP)
b. Model OAP-200X cloud particle spectrometer (CPS)
c. Model OAP-200Y precipitation particle spectrometer (PPS)

Each probe projects a collimated helium-neon laser beam normal to the airflow across a small sample area. In forward flight, particles passing through the beam (sample area) are counted and measured into 15 size classes per probe, each probe operating over a different size range. Functional airspeed range for the probes

Photo 1. Pressure Transducer Installed in Nozzle Receptacle to Measure Boom Air Pressure.

Photo 2. Thermocouple and Pressure Transducer Installed on a Water Manifold to Measure Boom Water Temperature and Pressure.

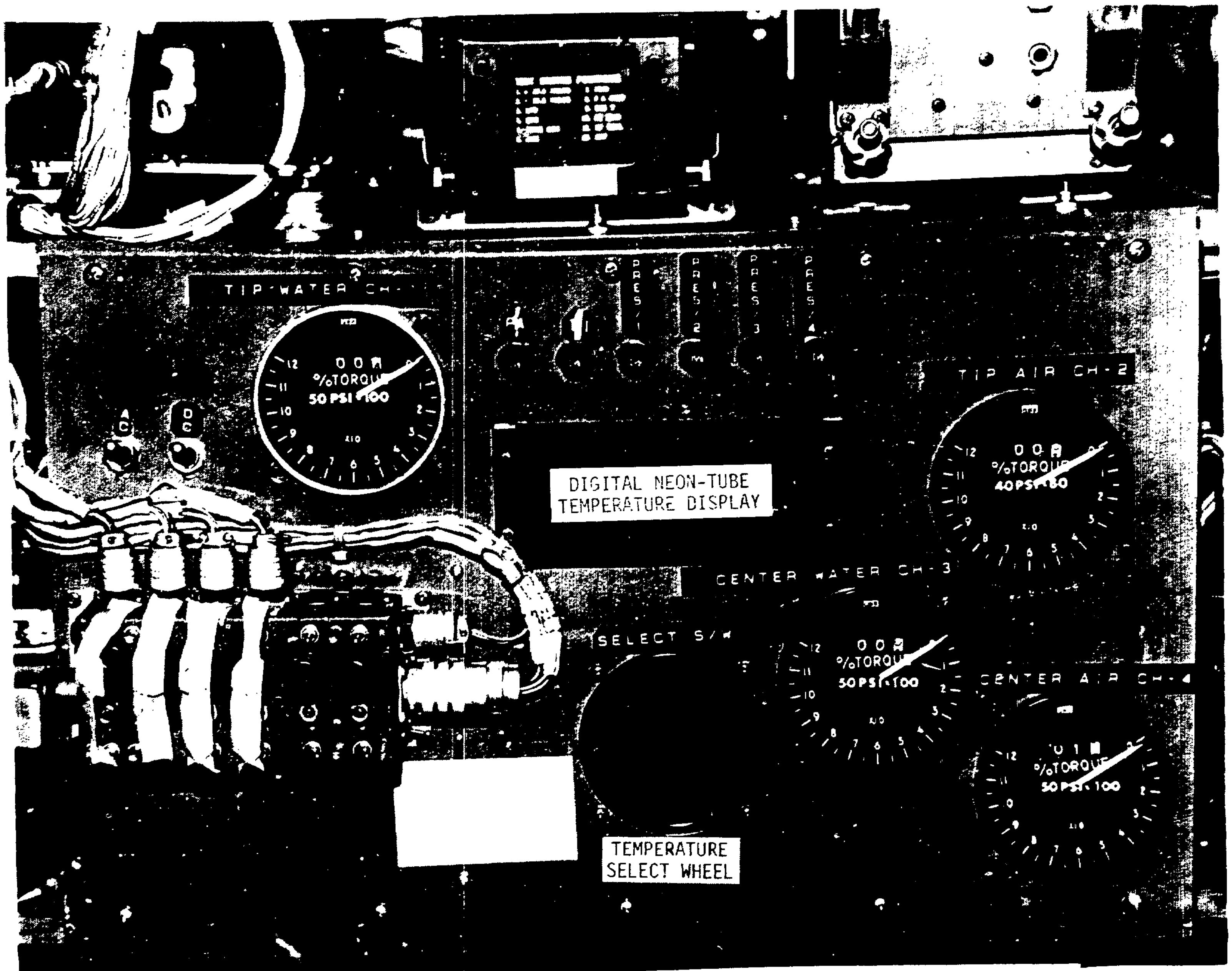

Photo 3. Control and Display Panel to Indicate Boom Air and Water Pressure and Temperature Measurements.

is 20 to 240 KTAS. The ASP operates on a light scattering technique, while the other two probes are of the optical array type. The ASP uses a photo detector module to measure intensity of forward scattered light from particles passing through the beam. In the ASP size range, scattered light intensity is a smooth function of particle size. Both the CPS and PPS focus the laser beam on a photodiode array, and particles crossing the beam cast a shadow over part of the array. The number of shadowed elements determines particle size. Both probes are similiar but operate over separate size ranges because of different photodiode arrays and magnification settings. Table 1 summarizes each probe as to particle size range and channel characteristics. The probes and their glass-bead calibrations are further described in Reference 7, Appendix A. Data reduction techniques for the probe measurements are described in Appendix D.

7. The probes were attached to brackets on either side of the measurement JUH-lH at cabin floor level near fuselage station 130. The ASP was mounted on the left side, and either the CPS or PPS on the right side. Horizontal distance between them was 10 ft. 10 in. Additional instrumentation and ice protection systems onboard the measurement JUH-1H are described in Reference 6, Appendix A.

TABLE 1. PARTICLE MEASURING PROBE SAMPLING CHARACTERISTICS

Probe*	Channel No.	Channel Midpoint (μm)	Channel Width (μm)	Sample Area (cm^2)
ASSP-100 AXIALLY SCATTERING PROBE	1	3	3	.00332
	2	6		
	3	9		
	4	12		
	5	15		
	6	18		
	7	21		
	8	24		
	9	27		
	10	30		
	11	33		
	12	36		
	13	39		
	14	42		
	15	45		
OAP-200X CLOUD PARTICLE SPECTROMETER	1	35	14	.0042
	2	49.5	15	.016
	3	64.7	15.4	.0343
	4	81.2	17.6	.058
	5	100	20	.0858
	6	120		.117
	7	140		.149
	8	160		.183
	9	180		.1708
	10	200		.1586
	11	220		.1464
	12	240		.134
	13	260		.122
	14	280		.1098
	15	300		.0976
OAP-200Y PRECIPITATION PARTICLE SPECTROMETER	1	140	140	15.4
	2	280		14.5
	3	420		13.7
	4	560		12.8
	5	700		12.0
	6	840		11.1
	7	980		10.2
	8	1120		9.39
	9	1260		8.54
	10	1400		7.69
	11	1540		6.83
	12	1680		5.98
	13	1820		5.12
	14	1960		4.27
	15	2100		3.42

*Probes manufactured by Particle Measurement Systems Inc.

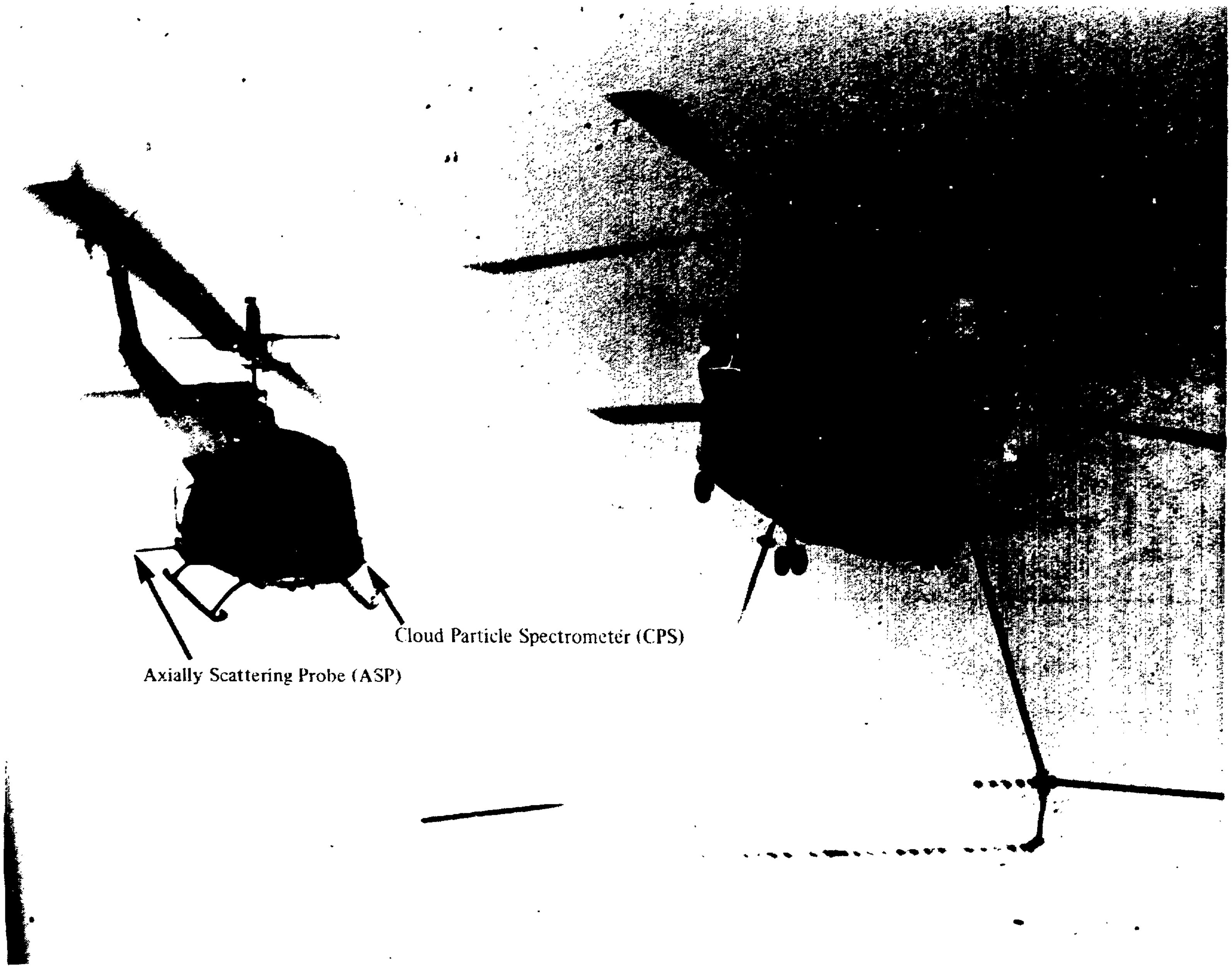

Photo 1. The *HISS* and *UH-1H* Measurement Aircraft Flying in Test Formation.

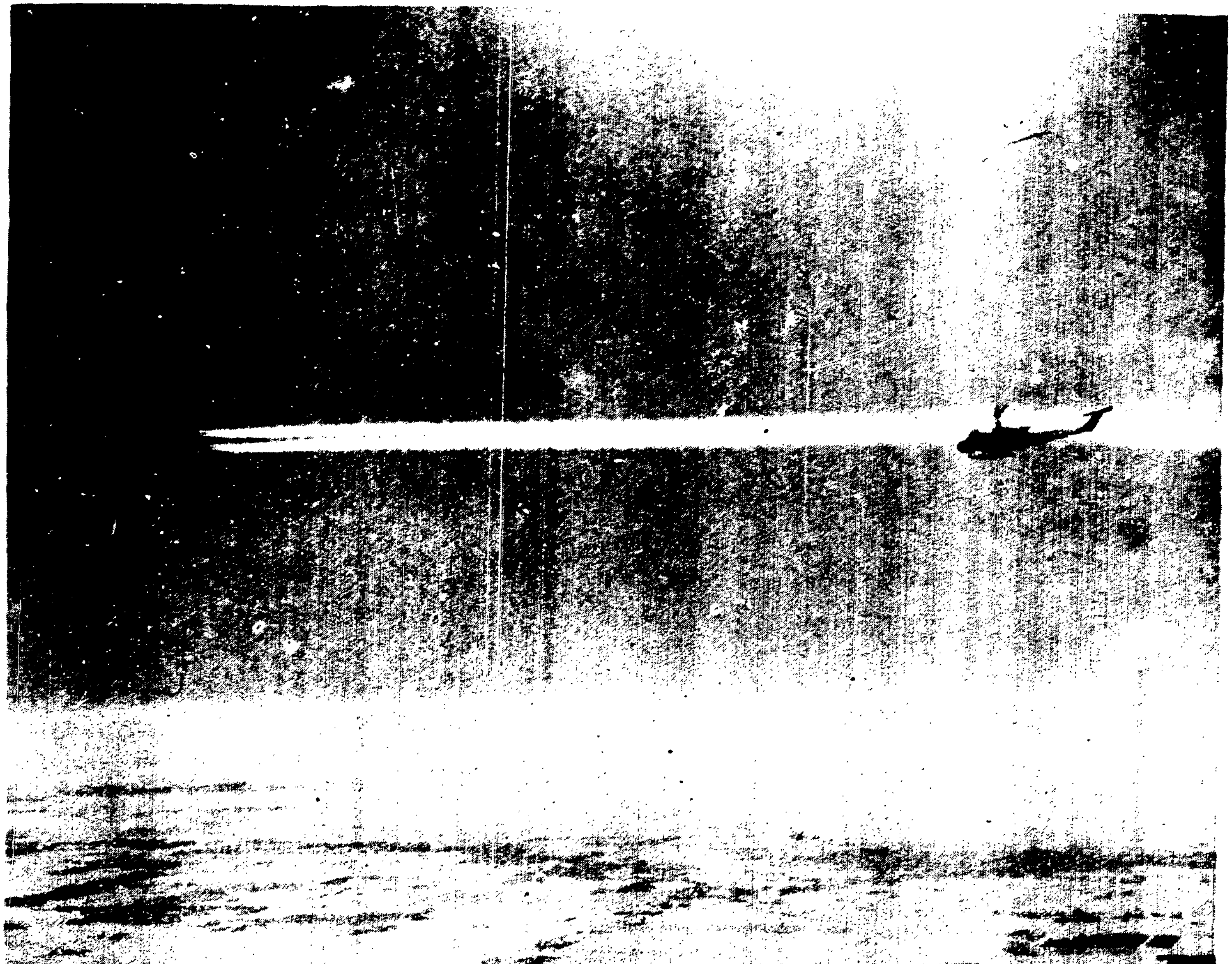

Photo 2. Side View of the HISS and UH-1H Measurement Aircraft Flying in Test Formation

APPENDIX D. TEST TECHNIQUES AND DATA ANALYSIS

TEST TECHNIQUES

1. The measurement JUH-1H aircraft equipped with MRI-furnished particle measuring spectrometers flew in formation behind the HISS and sampled the cloud by maneuvering to immerse the probes in the spray plume (Photo 1 and 2). A chase helicopter accompanied each flight to observe the measurement aircraft, assist in positioning, and provide airborne still and motion picture photography. All tests were flown at 90 KTAS, and standoff distances from the rear of the HISS, as measured by the radar altimeter, were varied from 150 to 300 ft.

2. Once the HISS had established a desired water flow rate from the spray boom, the measurement aircraft would perform both vertical and horizontal sweeps through the spray cloud, as well as stabilizing as long as 2 minutes with the probes held approximately centered in the cloud. This technique allowed assessing both vertical and horizontal variation of cloud parameters as well as measuring steady-state cloud-centered characteristics. Dimensions of the spray cloud were estimated by in-flight observation and photo comparison with known test aircraft dimensions.

3. The measurement aircraft initiated its vertical sweeps from a centered position beneath the cloud, climbing slowly until the probes were above the cloud, and then descending to the starting point. Horizontal sweeps were initiated from the center of the cloud, moving laterally to the left edge, followed by a sweep to the right. Returning to the starting point outside the cloud, the measurement aircraft would then perform additional sweeps or stabilize at points centered in the cloud.

DATA ANALYSIS

4. The MRI-furnished particle measuring probes, described in Appendix C, generate a continuous stream of 1-second samples. Each sample contains a particle number count and size classification into 15 separate channels per probe. All cloud paramaters are derived from the number count, size classification, and size of the air volume sampled, which depends on airspeed and probe type. A measured drop is assumed to lie in the center of its size class, although its actual diameter may fall anywhere within the channel. MRI combined data from the ASP and CPS probes into a spectral format presentation having 28 size classes covering drop diameters from 3 to 300 um. Selected 1-second samples were used to represent the cloud composition at each test condition.

5. Once the appropriate sample volume is used to normalize the number count in each channel on a "per cubic meter" basis, LWC can be calculated by summing the volumes of all the individual drops:

$$LWC = w \frac{4}{3} \pi \sum_{i=1}^{n} \left(\frac{D_i}{2}\right)^3 N_i$$

Where:

LWC = liquid water content ~ gm/m^3

W = density of liquid water ~ 1×10^6 gm/m^3

D_i = diameter of the ith channel ~ meters

N_i = number of drops in the ith channel per cubic meter

n = total number of size channels (28 in the spectral format)

Making this calculation for a single channel gives the LWC (drop mass) contained in drops of that size only. Dividing these number counts and drop masses per channel by channel width gives the number and mass concentrations as plotted in figures 7 and 8, Appendix E. On the 28-channel spectral format, channel width is 3 μm for drop diameters from 3 to 45 μm, and 20 μm for diameters from 60 through 300 μm. MRI software is used to calculate combined number counts in the 35 to 45 μm diameter range where ASP and CPS data overlap.

6. Median volumetric diameter (MVD) is the drop size which divides the volume of the spray in halves, such that half the total water volume is contained in drops larger and half in drops smaller than this median diameter. If the mass contained in each channel is first converted to a percentage of the total mass and these percentages are added consecutively, the MVD occurs at the diameter where the cumulative sum reaches 50%.

7. Mean volumetric diameter is the drop size whose volume is given by dividing the total mass of water by the total number of drops present. It can be calculated from the number count by:

$$\text{Mean volumetric diameter} = \left[\frac{\sum_{i=1}^{n} (N_i D_i^3)}{\sum_{i=1}^{n} N_i} \right]^{1/3}$$

The symbols are defined as in para 5, except the units for D (channel diameter) are microns (instead of meters) to calculate mean diameter in microns. This quantity does not appear on the spectral format listings furnished by MRI, but could be calculated from the information given.

8. MRI also performed a point-by-point analysis of consecutive 1-second samples for several vertical and horizontal sweeps to determine spatial variation of LWC and MVD within the cloud. The lack of precise spatial references for correlation with probe data during the sweeps required making two assumptions: (l) the measurement helicopter moved through the cloud at a constant rate, and (2) the cloud boundaries were defined when the probes stopped registering a significant number of drop counts (probes outside the cloud). These assumptions only permit an estimate of probe position relative to edges of the cloud, and do not provide data on actual cloud dimensions. Some discrepancies in the data could be expected for any given sweep because of cloud size relative to the measurement aircraft and the type of maneuver it performed while flying in formation. To overcome this, several sweep data sets were combined to best define general trends.

APPENDIX E. TEST DATA

INDEX

FIGURE
HELICOPTER ICING SPRAY SYSTEM
OPERATING AIR AND WATER PRESSURE

NOTE: Boom sensor locations shown in Appendix B

160 NOZZLES

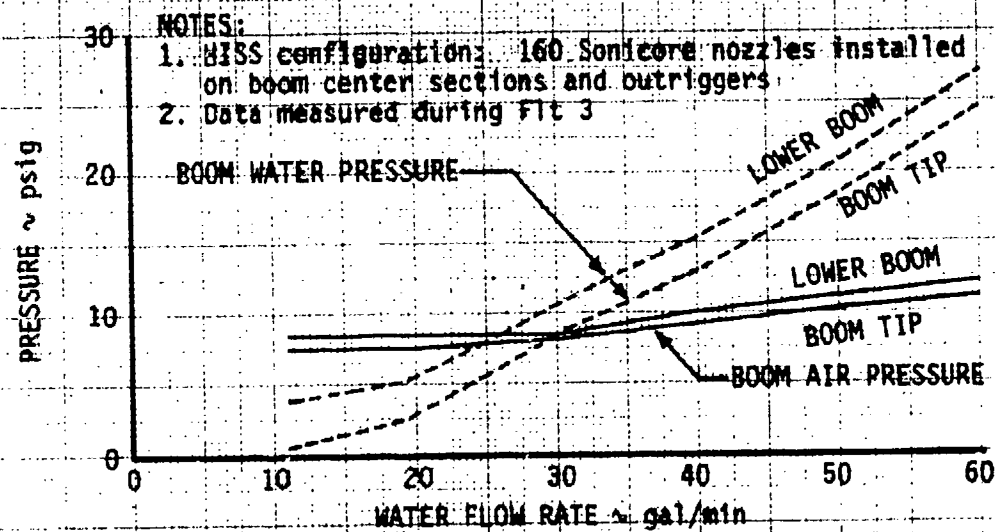

97 NOZZLES

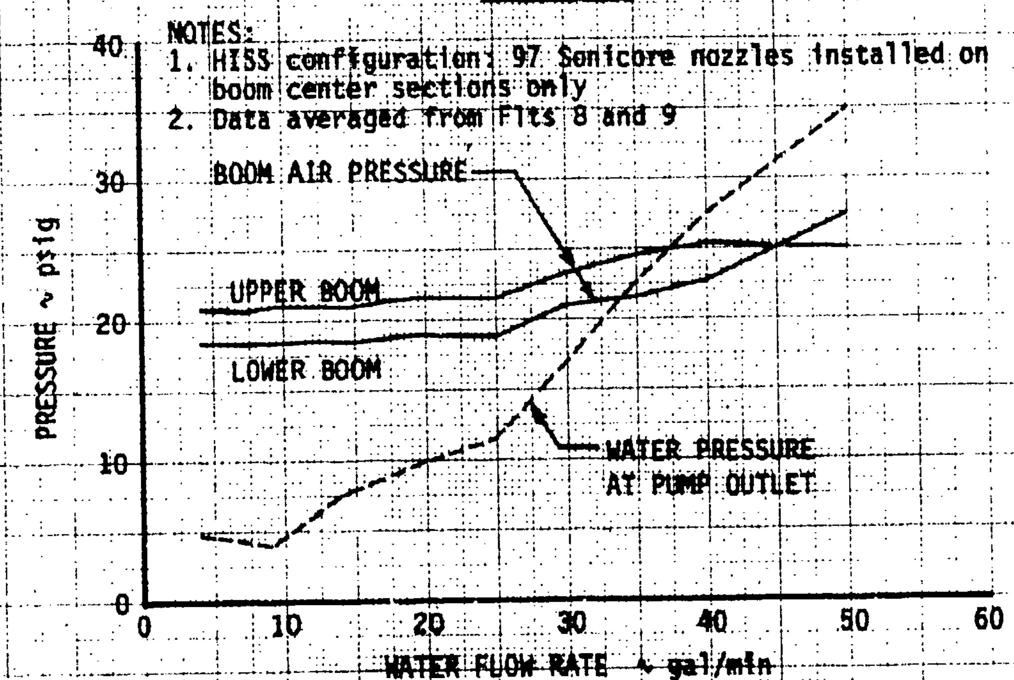

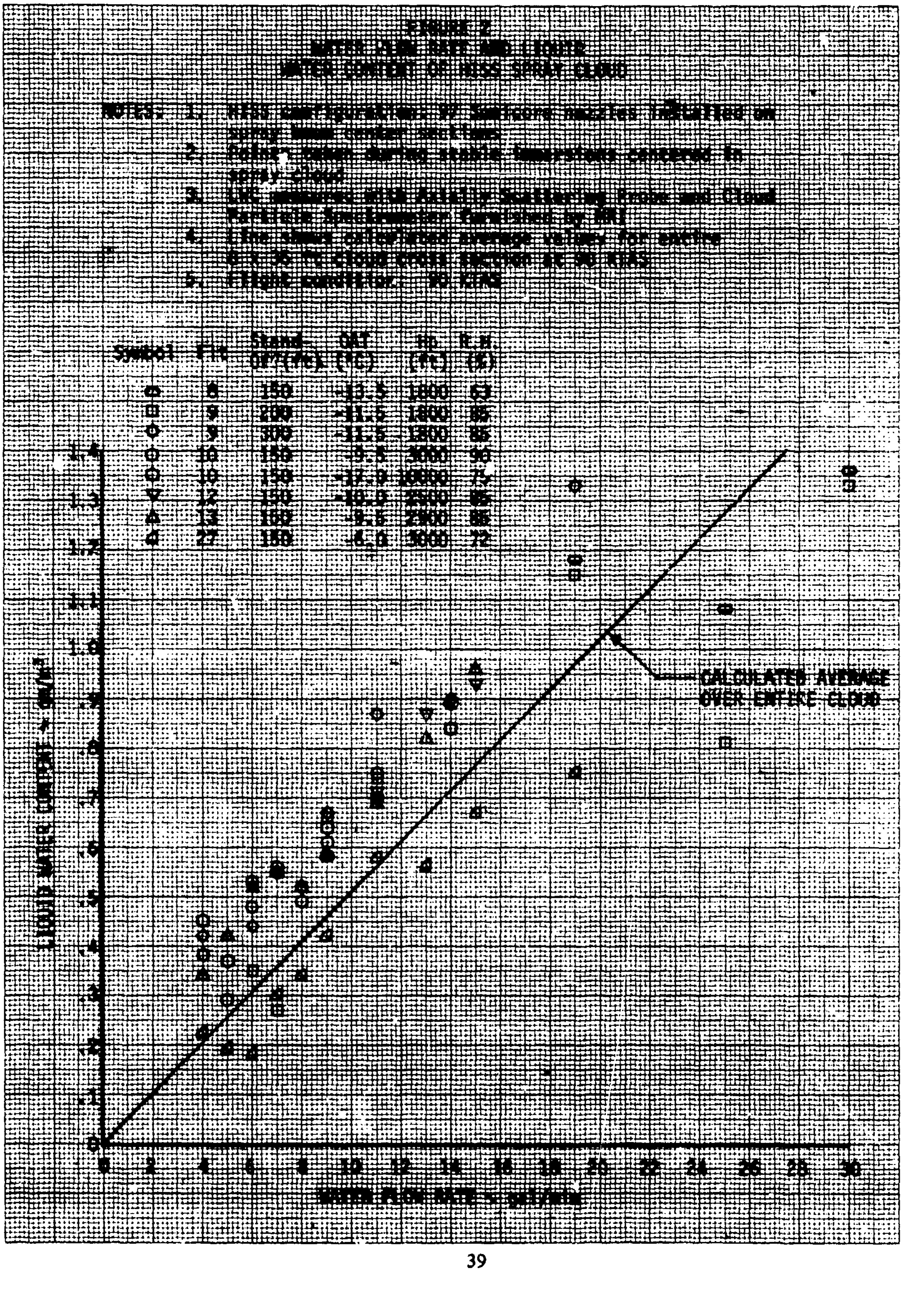
FIGURE 2
WATER FLOW RATE AND LIQUID
WATER CONTENT OF HISS SPRAY CLOUD
NOTES:
Symbol Flt Stand. OP (Psi) OAT (°C) Hp (ft) R.H. (%)
8 150 -13.5 1800 63
9 200 -11.5 1800 85
9 300 -11.5 1800 85
10 150 -9.5 3000 90
10 150 -17.0 10000 75
12 150 -10.0 2500 85
13 150 -9.5 2900 85
27 150 -6.0 3000 72
CALCULATED AVERAGE OVER ENTIRE CLOUD
LIQUID WATER CONTENT ~ gm/m³
WATER FLOW RATE ~ gal/min
0 .1 .2 .3 .4 .5 .6 .7 .8 .9 1.0 1.1 1.2 1.3 1.4
0 2 4 6 8 10 12 14 16 18 20 22 24 26 28 30

FIGURE 9
VERTICAL VARIATION OF LIQUID WATER
CONTENT WITHIN THE HESS SPRAY CLOUD

NOTES:
1. HESS configuration: 97 Sonicore nozzles installed on boom center sections only.
2. Data taken at 90 KTAS
3. Curves based on a collection of vertical sweep data from several flights.
4. Data scatter for each curve generally within ±.2 gm/m³ LWC
5. Curves shown do not represent exact values, but suggest average trends based on combined data.

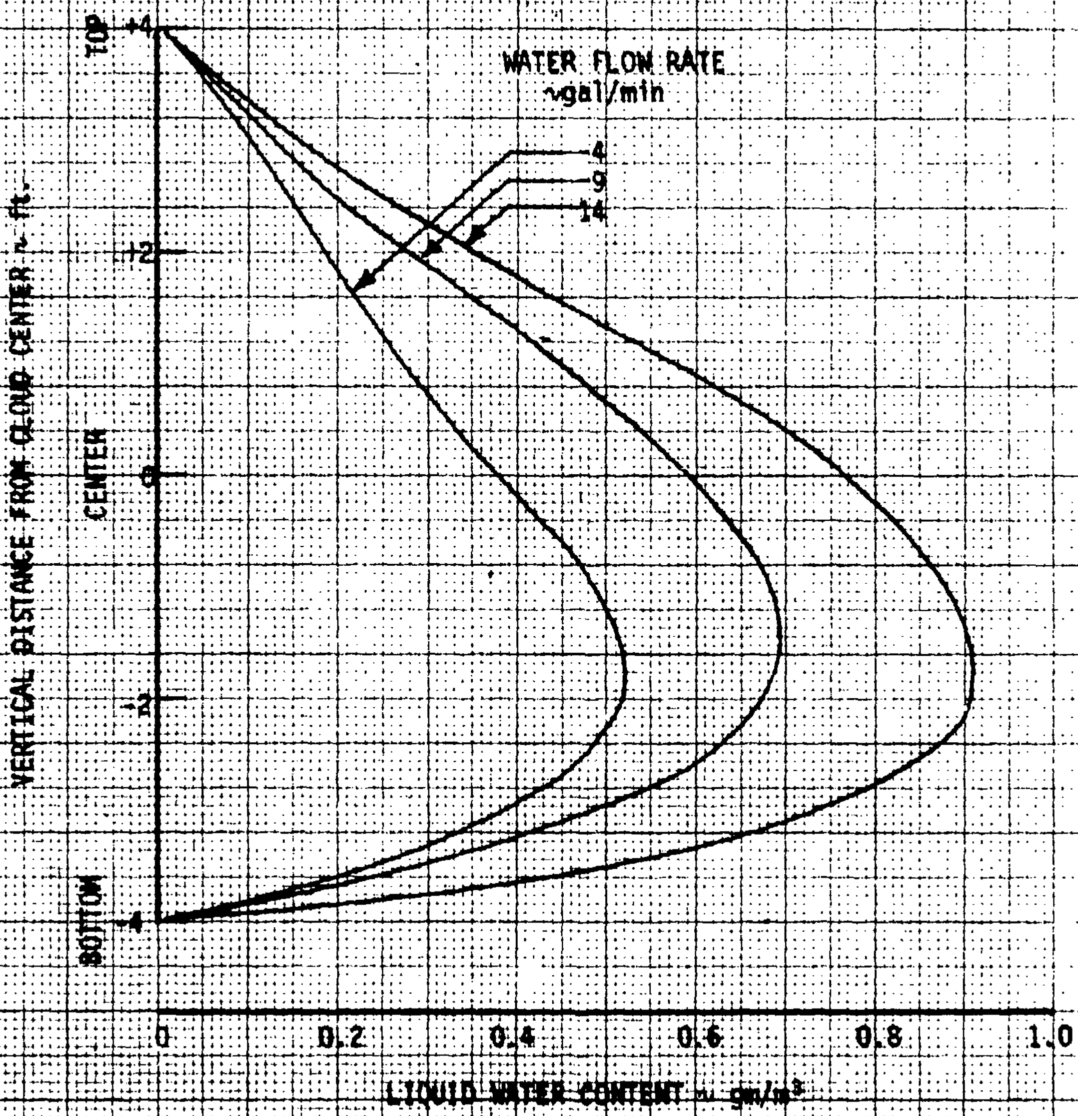

FIGURE 4
WATER FLOW RATE AND AVERAGE LIQUID
WATER CONTENT WITHIN DISCRETE SECTORS
OF THE HISS SPRAY CLOUD

NOTES:
1. HISS configuration: 97 Sonicore nozzles installed on boom center sections only
2. Curves based on data from Figure 3
3. LWC calculated by integrating vertical water distribution over defined horizontal layers
4. Curves drawn through incremental flow rate values of 4, 9, and 14 gal/min
5. Data taken at 90 KTAS
6. Straight line shows calculated average for entire 8 x 36 ft cloud cross section at 90 KTAS

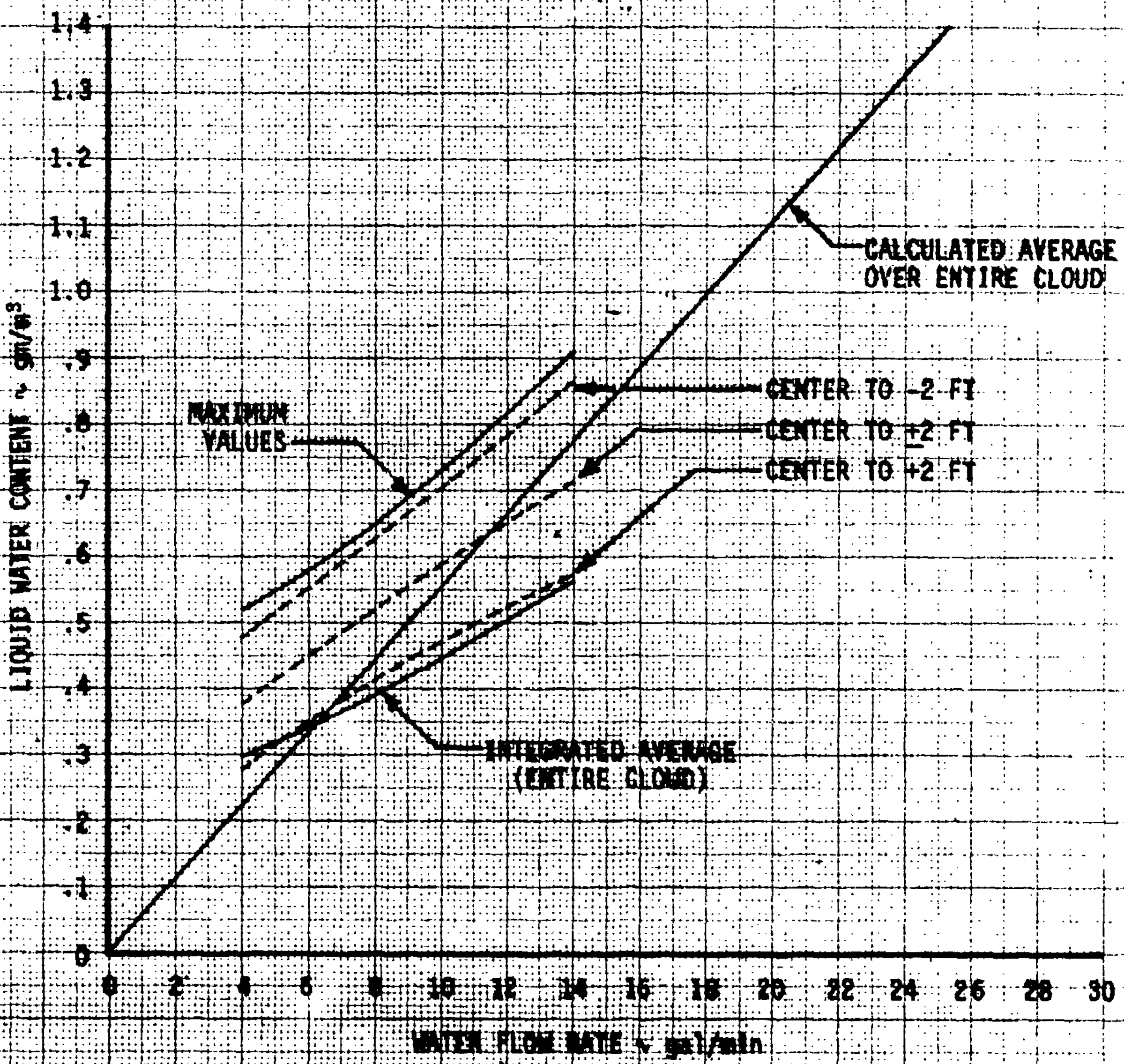

FIGURE 8
COMPARISON OF CLOUD DROP
MEDIAN VOLUMETRIC DIAMETER

NOTES:
1. Present HISS configuration: 97 Sonicore nozzles installed on boom center sections only
2. Previous HISS configuration: 91 All American Engineering Co. nozzles installed on boom center sections and outriggers
3. Data taken at 90 KTAS
4. HISS cloud depth estimated as 8 ft. in present configuration, 10 ft in previous configuration
5. MVD measured with Particle Measuring Spectrometers furnished by MRI
6. Ranges for HISS MVD values are based on combined vertical sweep data from several flights

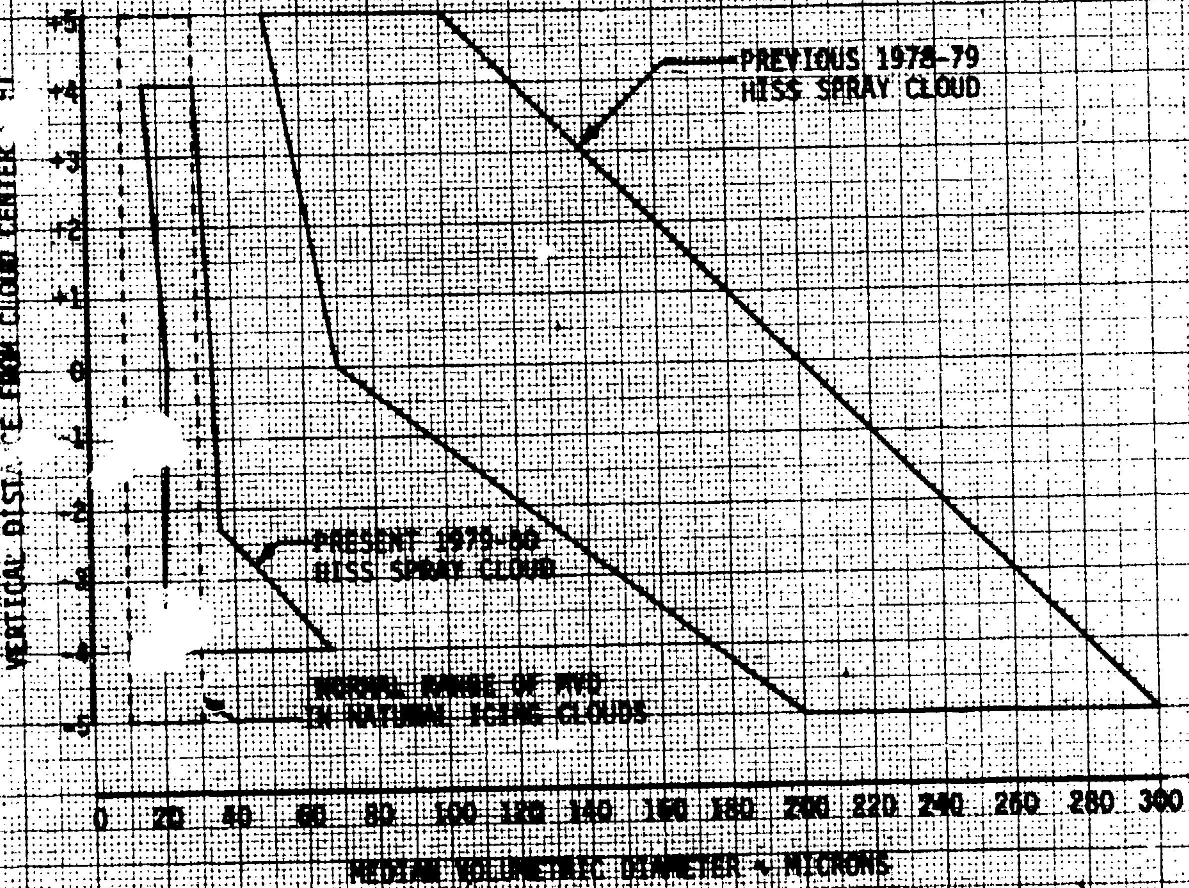

FIGURE 6

WATER FLOW RATE AND DROP SIZE MEDIAN VOLUMETRIC DIAMETER OF HISS SPRAY CLOUD

NOTES:
1. HISS configuration: 93 Sonicore nozzles installed on spray boom outer sections
2. Points taken during stable immersions centered in spray cloud
3. MVD measured with Axially Scattering Probe and Cloud Particle Spectrometer furnished by [illegible]
4. Dashed lines between Flt 9 data indicates order in which those 4 consecutive points were taken.
5. Flight condition: 90 KIAS

Symbol	Flt	Sepn Dist (Ft)	OAT (°C)	HP (Ft)	R.H. (%)
○	8	150	-13.5	1800	63
□	9	200	-11.5	1800	85
◇	9	300	-11.5	1800	85
○	10	150	-9.5	3000	90
○	10	180	-17.0	10000	75
▽	12	150	-10.0	2500	85
△	13	150	-9.5	2900	85

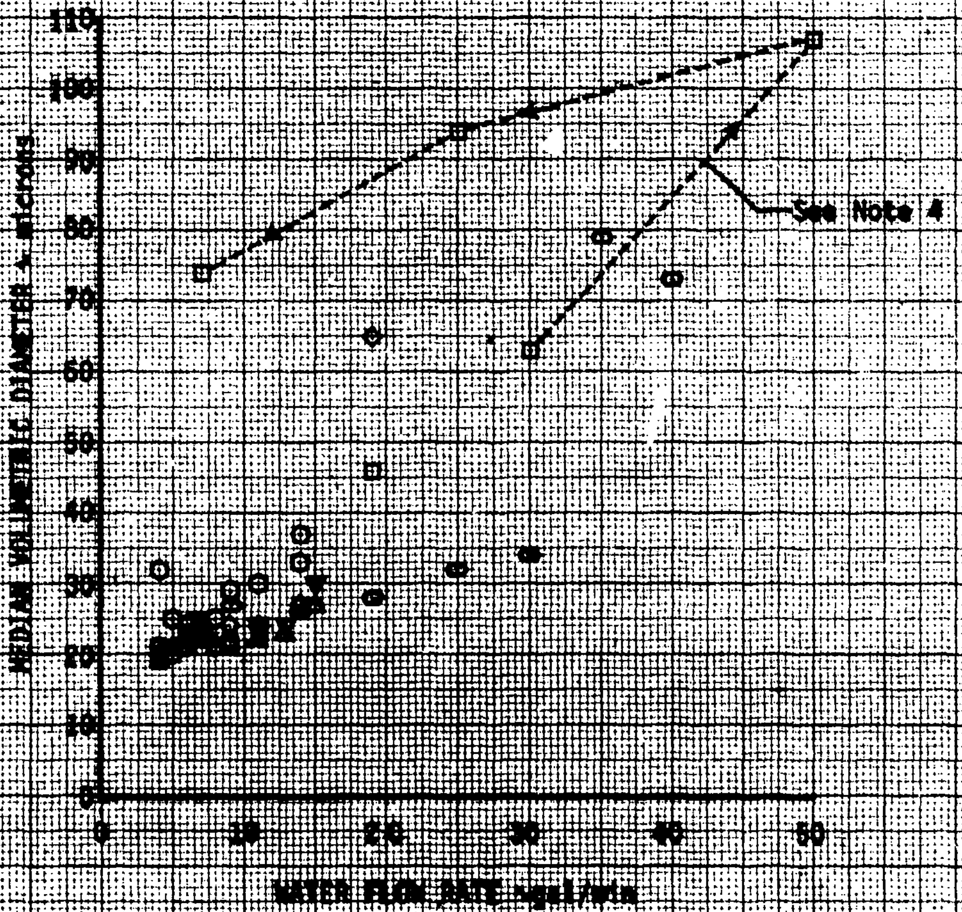

FIGURE 7
COMPARISON OF CLOUD
DROP NUMBER CONCENTRATION

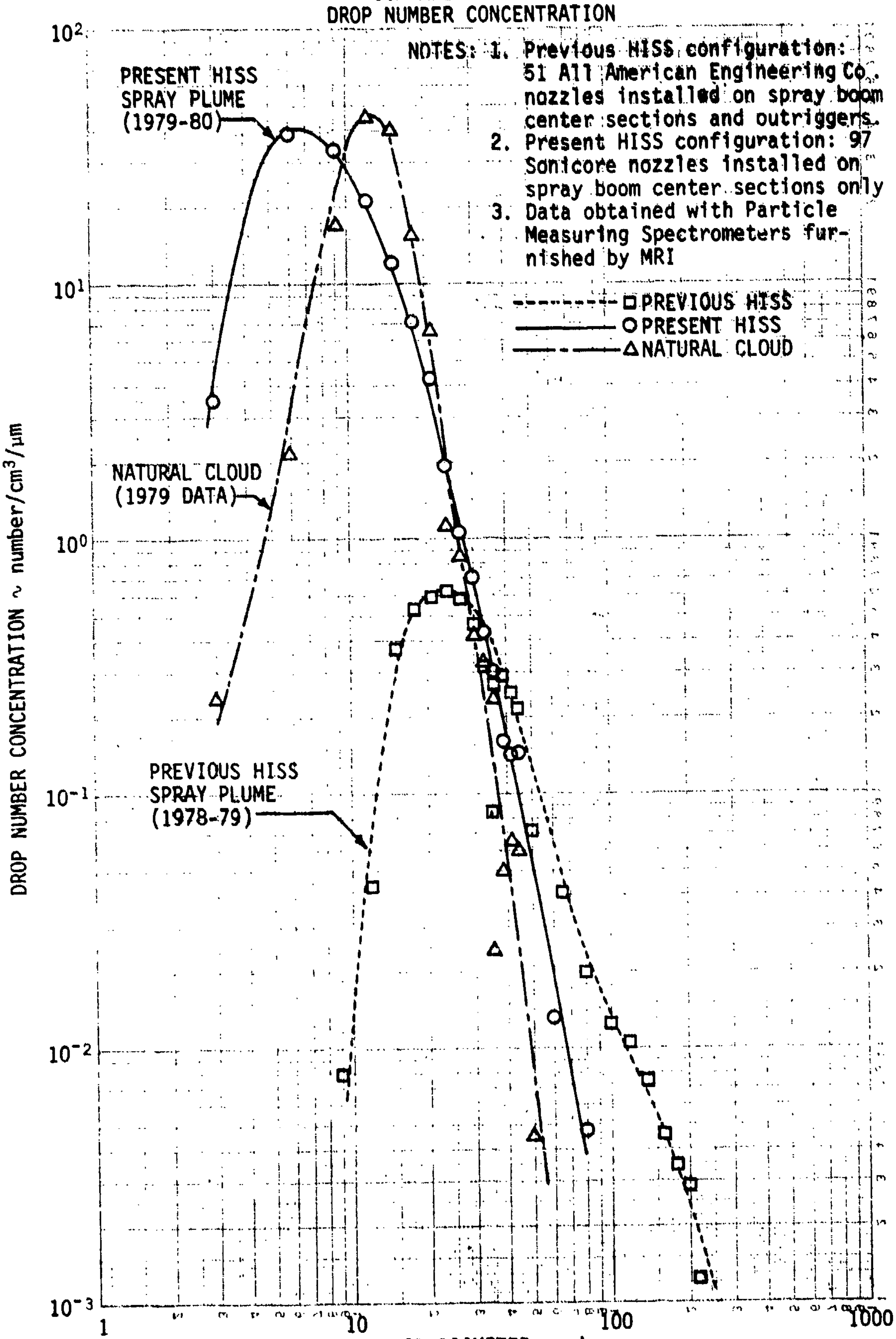

FIGURE 8
COMPARISON OF CLOUD
DROP MASS DISTRIBUTION

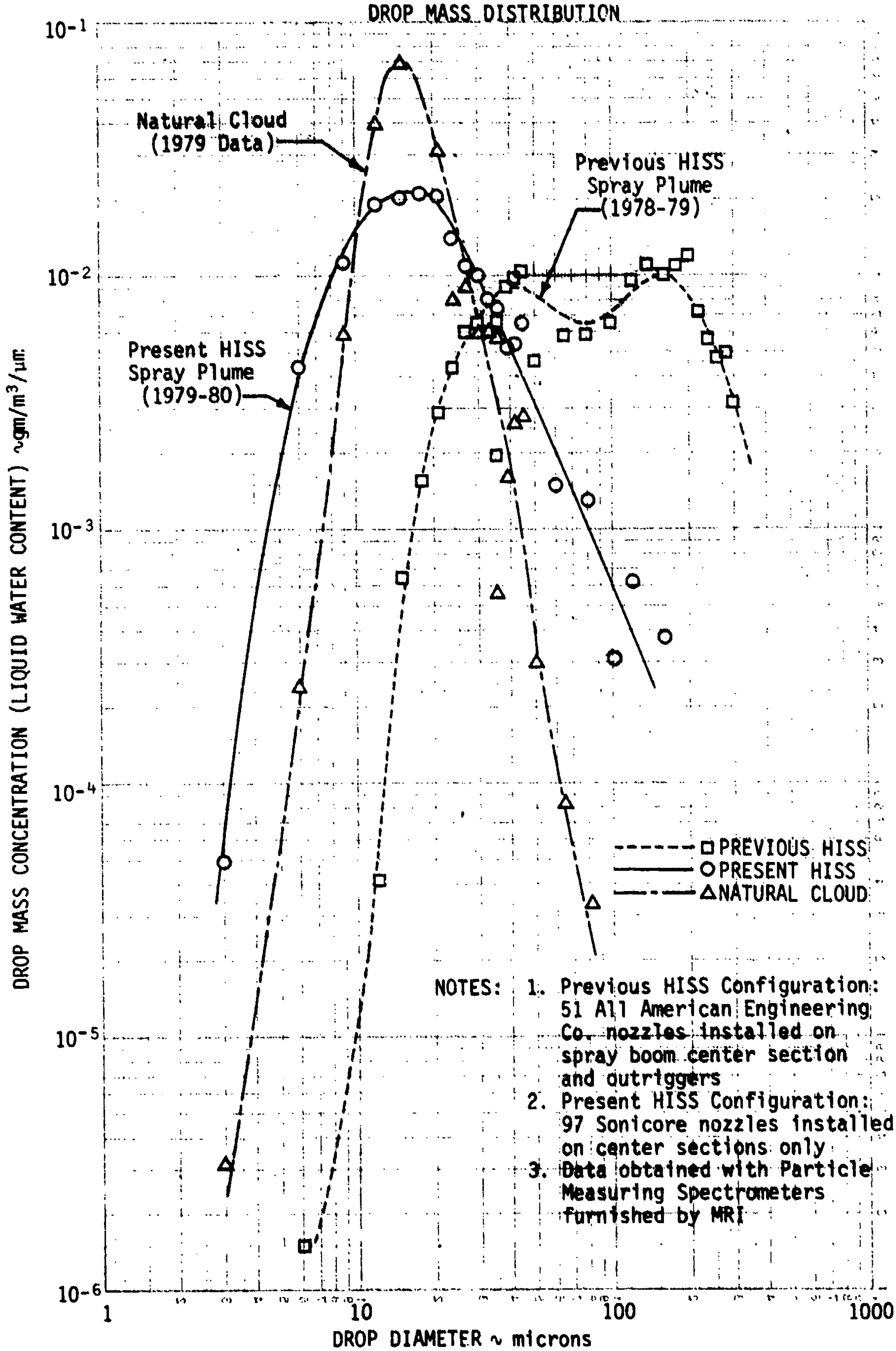

NOTES: 1. Previous HISS Configuration: 51 All American Engineering Co. nozzles installed on spray boom center section and outriggers
2. Present HISS Configuration: 97 Sonicore nozzles installed on center sections only
3. Data obtained with Particle Measuring Spectrometers furnished by MRI

DISTRIBUTION LIST

Deputy Chief of Staff for Logistics (DALO-SMM)	1
Deputy Chief of Staff for Operations (DAMO-RQ)	1
Deputy Chief of Staff for Personnel (DAPE-HRS)	1
Deputy Chief of Staff for Research Development and Acquisition (DAMA-PPM-T, DAMA-RA, DAMA-WSA)	3
Comptroller of the Army (DACA-EA)	1
US Army Materiel Development and Readiness Command (DRCDE-DH, DRCQA-E, DRCRE-I, DRCDE-RT)	4
US Army Training and Doctrine Command (ATTG-U, ATCD-T, ATCD-ET, ATCD-B)	4
US Army Aviation Research and Development Command (DRDAV-DI, DRDAV-EE, DRDAV-EG)	10
US Army Test and Evaluation Command (DRSTS-CT, DRSTS-AD)	2
US Army Troop Support and Aviation Materiel Readiness Command (DRSTS-Q)	1
US Army Logistics Evaluation Agency (DALO-LEI)	1
US Army Materiel Systems Analysis Agency (DRXSY-R, DRXSY-MP)	2
US Army Operational Test and Evaluation Agency (CSTE-POD)	1
US Army Armor Center (ATZK-CD-TE)	1
US Army Aviation Center (ATZQ-D-T, ATZQ-TSM-A, ATZQ-TSM-S)	3
US Army Combined Arms Center (ATZLCA-DM)	1
US Army Infantry Center (ATSH-TSM-BH)	1
US Army Safety Center (IGAR-TA, IGAR-Library)	2
US Army Research and Technology Laboratories/Applied Technology Laboratory (DAVDL-ATL-D, DAVDL-Library)	2
US Army Research and Technology Laboratories/Aeromechanics Laboratory (DAVDL-AL-D)	1

US Army Research and Technology Laboratories/Propulsion Laboratory (DAVDL-PL-D)	1
Defense Technical Information Center (DDR)	12
US Army Research and Technology Laboratories (DAVDL-ATL-ASA)	2
Federal Aviation Administration Technical Center (Contract Services Division, ANA-70)	50